Cyclitol secondary metabolism is a central feature of Burkholderia leaf symbionts

Bram Danneels, Monique Blignaut, Guillaume Marti, Simon Sieber, Peter Vandamme, Marion Meyer, Aurélien Carlier

TITLE : Cyclitol secondary metabolism is a central feature of *Burkholderia* leaf symbionts

Authors:

Danneels, Bram[1,2,*], Blignaut, Monique[3], Marti, Guillaume[4,5], Sieber, Simon[6], Vandamme, Peter[1], Meyer, Marion[3], Carlier, Aurélien[1,2,*]

[1] Laboratory of Microbiology, Department of biochemistry and microbiology, Ghent University, Ghent, Belgium

[2] LIPME, Université de Toulouse, INRAE, CNRS, 31320 Castanet-Tolosan, France

[3] Department of Plant Science, University of Pretoria, Pretoria, South Africa

[4] Metatoul-AgromiX Platform, LRSV, Université de Toulouse, CNRS, UT3, INP, Toulouse, France

[5] MetaboHUB-MetaToul, National Infrastructure of Metabolomics and Fluxomics, Toulouse, 31077, France

[6] Department of Chemistry, University of Zurich, 8057 Zurich, Switzerland.

[*] Co-corresponding author

Corresponding authors:

Bram Danneels: bram.danneels@inrae.fr

Aurélien Carlier: aurelien.carlier@inrae.fr

Abstract

The symbioses between plants of the Rubiaceae and Primulaceae families with *Burkholderia* bacteria represent unique and intimate plant-bacterial relationships. Many of these interactions have been identified through PCR-dependent typing methods, but there is little information available about their functional and ecological roles. We assembled seventeen new endophyte genomes representing endophytes from thirteen plant species, including those of two previously unknown associations. Genomes of leaf endophytes belonging to *Burkholderia s.l.* show extensive signs of genome reduction, albeit to varying degrees. Except for one endophyte, none of the bacterial symbionts could be isolated on standard microbiological media. Despite their taxonomic diversity, all endophyte genomes contained gene clusters linked to the production of specialized metabolites, including genes linked to cyclitol sugar analog metabolism and in one instance non-ribosomal peptide synthesis. These genes and gene clusters are unique within *Burkholderia s.l.* and are likely horizontally acquired. We propose that the acquisition of secondary metabolite gene clusters through horizontal gene transfer is a prerequisite for the evolution of a stable association between these endophytes and their hosts.

Introduction

Interactions with microbes play an important part in the evolution and ecological success of plants. For example, mycorrhizal associations are present in a vast majority of land plants, and the association with nitrogen-fixing bacteria provided legumes with an important evolutionary advantage (Brundrett, 1991; van Rhijn and Vanderleyden, 1995; Vessey *et al.*, 2005; Smith and Read, 2008). Nevertheless, microbes may also be harmful for plants as microbial pathogen interactions are responsible for major crop losses (Dangl and Jones, 2001; McCann, 2020). Many plant-microbe interactions only occur temporarily: contacts between microbes and the host are often limited to a sub-population or a specific developmental phase of the host. However, in some associations microbes are transferred from parents to offspring in a process called vertical transmission, resulting in permanent associations with high potential for co-evolution (Gundel *et al.*, 2017). While vertically-transmitted microbes are common in the animal kingdom, they have been more rarely described in plants (Fisher *et al.*, 2017).

A particular case of vertically transmitted microbes in plants are the bacterial leaf endophytes found in three different plant families: the monocot Dioscoreaceae, and the dicot Rubiaceae and Primulaceae. In the genera *Psychotria*, *Pavetta*, *Sericanthe* (Rubiaceae) and *Ardisia* (Primulaceae) this association may manifest in the form of conspicuous leaf nodules that house extracellular symbiotic bacteria (Miller, 1990; Van Oevelen *et al.*, 2002; Lemaire, Robbrecht, *et al.*, 2011; Lemaire, Van Oevelen, *et al.*, 2012; Ku and Hu, 2014). In some of these systems, the symbiont was detected in seeds, indicating that they can be transmitted vertically (Miller and Donnelly, 1987; Sinnesael *et al.*, 2018). Molecular analysis of the leaf nodules revealed that all endophytes are members of the *Burkholderia sensu lato*, more specifically to the newly defined *Caballeronia* genus (Van Oevelen *et al.*, 2002; Ku and Hu, 2014). Similar leaf endophytes, also belonging to the *Burkholderiaceae,* are present in Rubiaceae species that do not form leaf nodules, including some *Psychotria species* (Lemaire, Lachenaud, *et al.*, 2012; Verstraete *et al.*, 2013). To date, only one symbiont of Rubiaceae and Primulaceae has been cultivated: the endophyte of *Fadogia homblei*, which has been identified as *Paraburkholderia caledonica* (Verstraete *et al.*, 2011). Interestingly, members of *P. caledonica* are also commonly isolated from the rhizosphere or soil and have been detected in leaves of some *Vangueria* species (Verstraete *et al.*, 2014).

Speculations about possible functions of these leaf symbioses have long remained unsubstantiated because efforts to isolate leaf nodule bacteria or to culture bacteria-free plants were unsuccessful (Miller, 1990). Recently, sequencing and assembly of leaf symbiont genomes of several *Psychotria*, *Pavetta* or *Ardisia* species allowed new hypotheses about the ecological function of leaf symbiosis. Leaf symbiotic *Burkholderia* of *Ardisia crenata*, are responsible for the production of FR900359, a cyclic depsipeptide with potent bioactive and insecticidal properties (Fujioka *et al.*, 1988; Carlier *et al.*, 2016). Similarly, analysis of the genome of *Ca*. Burkholderia kirkii (*Ca*. B. kirkii), the leaf symbiont of *Psychotria kirkii*, revealed a prominent role of secondary metabolism (Carlier and Eberl, 2012). In this species, two biosynthetic gene clusters harboured on a plasmid encode two homologs of a 2-*epi*-5-*epi*-valiolone synthase (EEVS). EEVS are generally required for the production of cyclitol sugar analogs, a family of bioactive natural products with diverse targets (Mahmud, 2003, 2009). *Ca*. B. kirkii is likely involved in the synthesis of two cyclitol metabolites: kirkamide, a C_7N aminocyclitol with insecticidal properties, and streptol glucoside, a derivative of valienol

with broad allelopathic activities (Sieber *et al.*, 2015; Georgiou *et al.*, 2021). Similar gene clusters containing putative EEVS were also detected in the genomes of other *Psychotria* and a *Pavetta* leaf symbionts (Pinto-Carbó *et al.*, 2016), further highlighting the importance of cyclitol compounds in these leaf symbioses.

C_7 cyclitols are a group of natural products derived from the pentose phosphate pathway intermediate sedoheptulose-7-phosphate (SH7P) (Mahmud, 2003). Proteins of the sugar phosphate cyclase family are key enzymes in the synthesis of C_7 cyclitols. Enzymes of this family catalyse the cyclization of sugar compounds, an important step in primary and secondary metabolism (Wu *et al.*, 2007). Within this family, three main categories of enzymes use SH7P as a substrate: desmethyl-4-deoxygadusol synthase (DDGS), 2-*epi*-valiolone synthase (EVS) and 2-*epi*-5-*epi*-valiolone synthase (EEVS), of which EEVS is the only known enzyme involved in C_7N aminocyclitol synthesis (Osborn *et al.*, 2017). EEVS were originally only found in bacteria, where they catalyse the first step in the biosynthesis of C_7N aminocyclitol secondary metabolites (Mahmud, 2003; Sieber *et al.*, 2015). More recently, EEVS homologs have been discovered in some Eukaryotes such as fish, reptiles, and birds as well (Osborn *et al.*, 2015, 2017).

A second common feature of the leaf endophytes in Rubiaceae and Primulaceae is their reduced genomes. Leaf nodule *Burkholderia* symbionts of Rubiaceae and Primulaceae typically have smaller genomes than free-living relatives, as well as a lower coding capacity (Pinto-Carbó *et al.*, 2016). This reductive genome evolution is thought to be a result of increased genetic drift sustained in bacteria that are strictly host-associated, which leads to fixation of deleterious and/or neutral mutations and eventually to the loss of genes (Pettersson and Berg, 2007). This process is best documented in obligate insect symbionts such as *Buchnera* and *Serratia,* endosymbionts of aphids, or in *Sodalis*-allied symbionts of several insect groups (Shigenobu *et al.*, 2000; Toh *et al.*, 2006; Manzano-Marín *et al.*, 2018). Some of these symbionts have extremely small genomes and may present an extensive nucleotide bias towards adenosine and thymine (AT-bias) (Moran *et al.*, 2008). The process of genome reduction has multiple stages: first, recently host-restricted symbionts begin accumulating pseudogenes and insertion elements (McCutcheon and Moran, 2012; Lo *et al.*, 2016; Manzano-Marín and Latorre, 2016). Non-coding and selfish elements eventually get purged from the genomes over subsequent generations, which together with the general

deletional bias in bacteria results in a decrease in genome size (Mira *et al.*, 2001). This ultimately leads to symbionts with tiny genomes, with only a handful of essential genes necessary for survival or performing their role in the symbiosis. This process has been well documented in the leaf nodule symbionts of *Psychotria*, *Pavetta* and *Ardisia* species, but little is known about the genomes and functions of endophytes in species that do not form leaf nodules, notably Rubiaceae species of the *Vangueria* and *Fadogia* genera.

Here, we performed a comparative study of Rubiaceae and Primulaceae leaf endophytes from leaf nodulating and non-nodulating plant species using genomes assembled from shotgun metagenome sequencing data as well as isolates. We constructed a dataset of 26 leaf symbiont genomes (of which 17 new genomes from this study) from 22 plant species in 5 genera. All leaf symbionts show signs of genome reduction, in varying degree, and horizontal acquisition of secondary metabolite clusters is a universal phenomenon in these bacteria.

Material and Methods

Sample collection and DNA extraction

Leaves of Rubiaceae and Primulaceae species were freshly collected from different locations in South Africa or requested from the living collection of botanical gardens (Table S1). Attempts to isolate the endophytes were made for all fresh samples collected in South Africa (Table S1). Leaf tissue was surface sterilized using 70% ethanol, followed by manual grinding of the tissue in 0.4% NaCl. Supernatants were plated on 10% tryptic soy agar medium (TSA, Sigma) and R2A medium (Oxoid) and incubated at room temperature for 3 days or longer until colonies appeared. Single colonies were picked and passaged twice on TSA medium. Isolates were identified by PCR and partial sequencing of the 16S rRNA gene using the pA/pH primer pair (5'-AGAGTTTGATCCTGGCTCAG and 5'-AAGGAGGTGATCCAGCCGCA) (Edwards *et al.*, 1989). PCR products were sequenced using the Sanger method at Eurofins Genomics (Ebersberg, Germany).

DNA was extracted from whole leaf samples as follows. Whole leaves were ground in liquid nitrogen using a mortar and pestle. Total DNA was extracted using the protocol of Inglis et al. (Inglis *et al.*, 2018). Total DNA from a *Fadogia homblei* isolate was extracted following Wilson (Wilson, 2001). Sequencing library preparation and 2x150 paired-end metagenome

sequencing was performed by the Oxford Wellcome Centre for Human Genetics or by Novogene Europe (Cambridge, UK) using the Illumina NovaSeq 6000. Sequencing reads were classified using Kraken v2.1.2 against a custom database comprising complete prokaryotic and plastid genome sequences deposited NCBI RefSeq (accessed 4/4/2021), and visualised using KronaTools v2.7.1 (Ondov *et al.*, 2011; Wood *et al.*, 2019).

Bacterial genome assembly

Sequencing reads were trimmed and filtered using fastp v0.21.0 with default settings (Chen *et al.*, 2018). Overlapping paired-end reads were merged using NGmerge with default settings (Gaspar, 2018). For sequencing reads derived from new leaf samples, metagenome assemblies were created using metaSPAdes v3.15 on default settings but including the merged reads (Nurk *et al.*, 2017). Metagenomes were binned using Autometa, using a minimal contig length of 500 bp, taxonomy filtering (-m) and maximum-likelihood recruitment (using the -r option)(Miller *et al.*, 2019). Genome bins identified as *Caballeronia*, *Paraburkholderia*, or *Burkholderia* by Autometa were further assembled by mapping the original reads to these bins using smalt v0.7.6 (Ponsting and Ning, 2010). Mapped reads were extracted using samtools v1.9 (Li *et al.*, 2009) and reassembled using SPAdes v3.15 (Bankevich *et al.*, 2012) in default settings but using the --careful option, and binned again using Autometa. Contigs likely derived from eukaryotic contamination were removed after identification by blastn searches (e-value < $1e^{-6}$) against the NCBI nucleotide database (accessed January 2021) (Camacho *et al.*, 2009). Per-contig coverage information was calculated using samtools and contigs with less than 10% or more than 500% of the average coverage were manually investigated, and sequences likely derived from other bacterial or eukaryotic genomes were removed. Genome assembly for reads derived from isolates were assembled using Skesa v2.4.0 using default settings (Souvorov *et al.*, 2018). Assembly statistics were compiled using Quast v5.1.0 (Gurevich *et al.*, 2013).

To provide a more homogenous dataset for comparative genomics, Illumina read data for six previously published Rubiaceae symbionts, and the symbionts of *Ardisia crenata* and *Fadogia homblei* were re-assembled as above but using the published draft genomes as trusted contigs for both metaSPAdes and SPAdes assemblies (Table S2). The resulting assemblies were compared to the published assemblies using dotplots created by MUMmer (Marçais *et al.*, 2018). Genome assemblies of the symbionts of *Psychotria kirkii* (Carlier and

Eberl, 2012; Carlier *et al.*, 2013) and *Psychotria punctata* (Pinto-Carbó *et al.*, 2016) were downloaded from Genbank (Table S2). To assess whether the (re-)assembled genomes represent new species, genomes were analysed using TYGS (Type Strain Genome Server) (Meier-Kolthoff and Göker, 2019), and NCBI Blastn-based Average Nucleotide Identities (ANI) values calculated using the JSpecies web server (Richter *et al.*, 2016) and the pyANI python package (https://github.com/widdowquinn/pyani).

Genome annotation and pseudogene prediction

Assembled genomes were annotated using the online RASTtk pipeline (Brettin *et al.*, 2015), using GenemarkS as gene predictor, and locus tags were added using the Artemis software v18.1.0 (Carver *et al.*, 2012). Prediction of pseudogenes was performed using an updated version of the pseudogene prediction pipeline previously used for leaf symbionts (Carlier *et al.*, 2013). Briefly, orthologs of predicted proteins sequences of each genome in a dataset of published *Burkholderia* genomes (Table S3) were determined using Orthofinder v2.5.2 (Emms and Kelly, 2019) with default settings. The nucleotide sequences of each gene, including 200bp flanking regions, were aligned to the highest scoring sequence in each orthogroup using TFASTY v3.6 (Pearson, 2000). Genes were considered as pseudogenes if the alignment spanned over 50% of the query protein and the query protein contained a frameshift, or a nonsense mutation resulting in an uninterrupted alignment shorter than 80% of the target sequence. Moreover, ORFs were classified as non-functional if at least one of the following criteria was true: amino acid sequence shorter than 50 residues which did not cluster in an orthogroup, and sequence without any significant blastx hit against the reference database (e-value cut off = 0.001); proteins without predicted orthologs in the *Burkholderia* dataset, but which showed a blastx hit against the reference set in an alternative reading frame; and finally proteins without any hit in the *Burkholderia* genome database or in the NCBI nr database. Blastx and blastp searches were performed using DIAMOND v2 (Buchfink *et al.*, 2021). For the genomes of the symbionts of *P. kirkii* and *P. punctata* the original gene and pseudogene predictions were used. Insertion elements in both newly assembled and re-assembled genomes were predicted using ISEscan v1.7.2.3 with default settings (Xie and Tang, 2017).

Phylogenetic analysis

16S rRNA sequences were extracted from the endophyte (meta)genomes using Barrnap v0.9 (https://github.com/tseemann/barrnap). For genomes where no complete 16S rRNA could be detected, reads were mapped to the 16S rRNA gene of the closest relative with a complete 16S rRNA sequence. These reads were assembled using default SPAdes (Prjibelski *et al.*, 2020) using the --careful option. Near complete (>95%) 16S rRNA sequences could be extracted using these methods, except for the hypothetical endophyte of *Pavetta revoluta*. The 16S rRNA sequences were identified using the EzBiocloud 16S rRNA identification service (https://www.ezbiocloud.net/identify). Phylogenetic analysis of the leaf endophytes and *Burkholderia s.l.* genomes was performed using the UBCG pipeline v3.0 (Na *et al.*, 2018). The pipeline was run using the default settings, except for the gap-cutoff (-f 80). The resulting superalignment of 92 core genes was used for maximum-likelihood phylogenetic analysis using RAxML, using the GTRGAMMA evolution model, and performing 100 bootstrap replications (Stamatakis, 2014). Plastid reference alignments were created using Realphy v1.12 using standard settings and the *Coffea arabica* chloroplast genome (NCBI accession NC_008535.1) as reference (Bertels *et al.*, 2014). Published chloroplast genomes of *Ardisia mamillata* (NCBI accession MN136062), *Psychotria kirkii* (NCBI accession KY378696), *Pavetta abyssinica* (NCBI accession KY378673), *Pavetta schumanniana* (NCBI Accession MN851271), and *Vangueria infausta* (NCBI accession MN851269) were also included in the alignment. Phylogenetic trees were constructed using PhyML v3.3.3 with automatic model selection, and 1000 bootstrap replicates (Guindon *et al.*, 2010). For plant species with uncertain taxonomic identification, seven plant markers were extracted by blastn searches against the metagenome: ITS, nad4, rbcL and rpl16 of *Pavetta abyssinica* (NCBI accessions MK607930.1, KY492180.1, Z68863.1, and KY378673.1), matK from *Pavetta indica* (NCBI accession KJ815920.1), petD from *Pavetta bidentata* (NCBI accession JN054223.1), and trnTF from *Pavetta sansibarica* (NCBI accession KM592134.1).

Core-genome phylogenies of symbiont genomes were constructed by individually aligning the protein sequences of all single-copy core genes using MUSCLE, back-translating to their nucleotide sequence using T-Coffee v13.45 (Di Tommaso *et al.*, 2011), and concatenating into one superalignment. Maximum-likelihood phylogenetic analysis was performed using RAxML, using the GTRGAMMA evolution model, 100 bootstrap replicates, and using

partitioning to allow the model parameters to differ between genes. Phylogenetic trees were visualised and edited using iTOL (Letunic and Bork, 2019).

Comparative genomics

Ortholog prediction between leaf symbiont genomes and a selection of reference genomes of the *Burkholderia, Paraburkholderia* and *Caballeronia* genera (BPC-set; selected using NCBI datasets tool (https://www.ncbi.nlm.nih.gov/datasets/genomes); Table S3) was performed using Orthofinder v2.5.2 using default settings (Emms and Kelly, 2019). Core genome overlap was visualised in Venn diagrams using InteractiVenn (Heberle *et al.*, 2015). Non-essential core genes were identified by blastp searches against the database of essential genes (DEG)(Zhang, 2004), identifying as putative essential genesORFs with significant matches in the database (e-value < $1e^{-6}$). Standardised functional annotation was performed using eggNOG-mapper v2.1.2 (Huerta-Cepas *et al.*, 2019; Cantalapiedra *et al.*, 2021). Enrichment of protein families in leaf symbiont genomes was determined by comparing the proportion of members of leaf symbionts and the BPC-set in orthogroups. Enriched KEGG pathways were identified by comparing the average per-genome counts of genes in every pathway between leaf symbiont genomes and genomes from the BPC-set. Presence of motility and secretion system clusters was investigated using the TXSScan models implemented in MacSyFinder (Abby *et al.*, 2014, 2016). Homologues of the *Ca.* B. kirkii putative 2-*epi*-5-*epi*-valiolone synthase (EEVS) were identified by blastp searches against the proteomes of the leaf symbiont genomes (e-value cut-off: $1e^{-6}$). Putative EEVS genes were searched against the SwissProt database, and functional assignment was done by transferring the information from the closest match within the sugar phosphate cyclase superfamily (Schneider *et al.*, 2004; Osborn *et al.*, 2017). Contigs containing these genes were identified and extracted using Artemis, and aligned using Mauve (Lòpez-Fernàndez *et al.*, 2015). Gene phylogenies were constructed by creating protein alignments using MUSCLE followed by phylogenetic tree construction using FastTree (Price *et al.*, 2009), including the protein sequences of three closely related proteins in other species, determined by blastp searches against the RefSeq protein database (accessed July 2021).

The data generated in this study have been deposited in the European Nucleotide Archive (ENA) at EMBL-EBI under accession number PRJEB52430 (https://www.ebi.ac.uk/ena.browser/view/PREJB52430).

Results

Detection and identification of leaf endophytes

To gain insight into potential association of various Primulaceae and Rubiaceae species with *Burkholderia s.l.* endosymbionts, we collected samples from 16 Rubiaceae (1 *Fadogia* sp., 5 *Pavetta* spp., 2 *Psychotria* spp., and 8 *Vangueria* spp.) and 3 Primulaceae (3 *Ardisia* spp.) species (Table S1). We extracted DNA from entire leaves and submitted the samples to shotgun sequencing without pre-processing of the samples to remove host or organellar DNA. We found evidence for endophytic *Burkholderia* in 14 out of 19 species investigated (Table S1). In these samples, the proportion of sequencing reads identified as *Burkholderiaceae* ranged from 5% to 57% of the total, except for the *Pavetta revoluta* sample (0.4%) and 1 of 2 *Vangueria infausta* samples (0.9%). Analysis of 16S rRNA sequences revealed 100% pairwise identity over 1529 bp suggesting that the same endophyte species was present in both *V. infausta* samples. In *Pavetta revoluta*, the closest relative of the leaf endophyte based on 16S rRNA sequence similarity was *Caballeronia calidae* (98.89% identity over 808 bp; Table S1). Of the nine species with significant amounts of *Burkholderia* s.l. reads and for which isolation attempts were made (Table S1), only the endophyte of *Fadogia homblei* could be cultured (isolate R-82532). Leaf samples of four species (*Psychotria capensis*, *Psychotria zombamontana*, *Pavetta ternifolia*, and *Pavetta capensis*) contained low amounts of bacterial DNA (<2% of reads), and likely do not have stable symbiotic endophyte associations. Seven percent of the reads obtained from the *Pavetta indica* sample were classified as bacterial, but with a diverse range of taxa present indicating possible contamination with surface bacteria (Figure S1). Plastid phylogenies indicated that samples attributed to *Pavetta capensis* and *Pavetta indica* did not cluster with other *Pavetta* species (Figure S2). Analysis of genetic markers revealed that our *Pavetta indica* sample was likely a misidentified *Ixora* sp. Analysis of *Pavetta capensis* marker genes revealed the specimen is likely part of the Apocynaceae plant family, with a 100% identity match against the *rbcL* sequence of *Pleiocarpa mutica.* These samples were not taken into account in further analyses.

Analysis of the 16S rRNA sequences extracted from metagenome-assembled genomes (MAGs) identified all leaf endophytes as *Burkholderia s.l.* (Table S1). Phylogenetic analysis shows that all endophytes of *Psychotria, Pavetta*, and *Ardisia* cluster within the genus

298 *Caballeronia*, while the endophytes of *Vangueria* and *Fadogia* belong to the
299 *Paraburkholderia* genus (Figure 1A). All endophytes of *Ardisia* are closely related to each
300 other and form a clade with *Caballeronia udeis* and *Caballeronia sordidicola*. Based on the
301 commonly used ANI (95-96%) cut-off, these endophytes are separate species from *C. udeis*
302 and *C. sordidicola* (ANI <94%; 16S rRNA sequence identity <98.4). The endophytes of *Ardisia*
303 *crenata* and *Ardisia virens* are very closely related and belong to the same species: *Ca.*
304 Burkholderia crenata (ANI >99%; 16S rRNA sequence identity 99.8%) (Table S4). Similarly,
305 the endophytes of *Ardisia cornudentata* and *Ardisia mamillata* belong to the same species
306 (ANI = 95.56%), which we tentatively named *Ca.* Burkholderia ardisicola (species epithet
307 from *Ardisia*, the genus of the host species, and the Latin suffix - *cola* (from L. n. *incola*),
308 dweller, see species description in Supplementary Information). Endophytes of *Psychotria*
309 and *Pavetta* are scattered across the *Caballeronia* phylogeny, but all are taxonomically
310 distinct from free-living species (Figure 1A; ANI <93% with closest non-endophyte relatives).
311 Each of these endophytes also represents a distinct bacterial species with pairwise Average
312 Nucleotide Identity (ANI) values below the commonly accepted species threshold of 95-96%,
313 except for *Ca.* P. schumanniana and *Ca.* B. kirkii whose genomes share 95.65% ANI (Table
314 S4). The endophytes of *Vangueria* and *Fadogia* form three distinct lineages of
315 *Paraburkholderia*. The endophytes of *Vangueria dryadum* and *Vangueria macrocalyx* are
316 nearly identical (ANI >99.9%; identical 16S rRNA), but do not belong to any known
317 *Paraburkholderia* species (ANI <83% with closest relative *Paraburkholderia* species). We
318 tentatively assigned these bacteria to a new species which we named *Ca. Paraburkholderia*
319 *dryadicola* (from a Dryad, borrowed from the species epithet of one of the host species, and
320 Latin suffix – *cola*, see species description in Supplementary Information). Similarly, the
321 endophytes of *V. infausta*, *V. esculenta*, *V. madagascariensis*, *V. randii*, and *V.*
322 *soutpansbergensis* cluster together with *Paraburkholderia phenoliruptrix* (Figure 1A). While
323 the endophyte of *Vangueria soutpansbergensis* forms a separate species (named here *Ca.*
324 *Paraburkholderia soutpansbergensis;* ANI <95% with *P. phenoliruptrix*) the other endophytes
325 fall within the species boundaries of *P. phenoliruptrix*. (ANI 95-96% between these
326 endophytes and *P. phenoliruptrix*). Lastly, the endophytes of *Fadogia homblei* and *Vangueria*
327 *pygmaea* showed identical 16S rRNA sequences, and clustered with *Paraburkholderia*
328 *caledonica*, *P. strydomiana*, and *P. dilworthii* (Figure 1A). Similarly high ANI values (>97.5%)
329 and 16S rRNA sequence similarity (>99.7%) ambiguously fall within the species boundaries of

both *P. caledonica* and *P. strydomiana*. Because endophytes of *F. homblei* were previously classified as *P. caledonica* (Verstraete *et al.*, 2011, 2014), we propose classifying the endophytes of *F. homblei* and *V. pygmaea* as members of *P. caledonica*, and consider *P. strydomiana* a later heterotypic synonym of *P. caledonica*.

Phylogenetic analysis based on the core genomes of endophytes indicates a general lack of congruence with the host plant phylogeny (Figure S3). Endophytes of *Ardisia* are monophyletic within the *Caballeronia* genus and follow the host phylogeny. In contrast, endophytes of *Pavetta* are not monophyletic and are nested within the *Psychotria* endophytes. Similarly, the *Fadogia homblei* endophyte clusters with endophytes of *Vangueria*.

Leaf endophyte genomes show signs of genome reduction.

We could assemble nearly complete bacterial genomes for all samples where we detected *Burkholderia* endophytes, except for those of the *Pavetta revoluta* and one *Vangueria infausta* sample with too few bacterial reads. Binning analysis grouped endophyte sequences in a single bin per sample, with high completeness (>95%) and purity (>97%). Most assemblies ranged between 3.5 and 5 Mbp in size, with 2 outliers: 2.58 Mbp for *Ca.* B. crenata Avir, and 8.92 Mbp for *P. caledonica* R-49542 (Table 1). The %G+C of all genomes fell in the range of 59-64 %G+C, which is within the range of free-living *Paraburkholderia* and *Caballeronia* genomes (Vandamme *et al.*, 2017). All genomes showed signs of ongoing genome reduction. Because of rampant null or frameshift mutations, a large proportion of predicted CDS code for non-functional proteins. As a result, coding capacity is low for all endophyte genomes varying between 83% in *P. caledonica* R-49542 and 40% in *Ca.* B. ardisicola Acor (Figure 1B, Table 1). In addition, insertion sequence (IS) elements make up a large amount of the genomes: 1.97% of the assembly size on average, but up to almost 10% in some symbionts of *Psychotria* (Table 1). Reassembly of previously investigated endophytes of *Psychotria* and *Pavetta* yielded genomes of similar size to the original assemblies, except for Ca. *Burkholderia schumanniana*. The original genome assembly size was estimated at 2.4 Mbp, while our reassembly counted 3.62 Mbp. A dot plot between both assemblies indicated that the size discrepancy is not solely due to differential resolution of repeated elements (Figure S4). Thus, our new assembly includes 1.2 Mbp of genome sequence that was missed in the original assembly.

Burkholderia leaf endophytes in Rubiaceae and Primulaceae shared a core genome of 607 genes (Figure S5). Even within specific phylogenetic lineages the core genomes were small: 774 genes in endophytes belonging to the *Caballeronia* symbionts of *Psychotria* and *Pavetta*, 1001 genes in endophytes of *Caballeronia* symbionts of *Ardisia*, and 1199 in *Paraburkholderia* endophytes of *Fadogia* and *Vangueria*. This corresponds to 29.5%, 52.4%, and 28.4% of the average functional proteome for each species cluster, respectively. Only 28 proteins of the total core genome did not show significant similarity with proteins from the database of essential genes (Table S5). Eleven of these proteins have unknown functions and a five are membrane-related. Fifteen genes of the endophyte core genome did not have orthologs in >95% of related *Burkholderia*, *Caballeronia*, and *Paraburkholderia* genomes (Table S6). No COG category was specifically enriched in this set of proteins.

Because secretion of protein effectors is often a feature of endophytic bacteria (Brader *et al.*, 2017), we searched for genes encoding various secretion machineries in the genomes of *Burkholderia* endophytes. Flagellar genes, as well as Type III, IV or VI secretion system were not conserved in all leaf endophytes (Figure S6). The most eroded symbionts of *Psychotria*, *Pavetta,* and *Ardisia* lack almost all types of secretion systems, and most also lack a functional flagellar apparatus. Type V secretion systems are present in *Ca.* Burkholderia ardisicola Acor, *Ca.* B. pumila, and *Ca.* B. humilis. The genomes of *Paraburkholderia* symbionts of *Vangueria* and *Fadogia* were generally richer in secretions systems, but only T1SS and T2SS are conserved. A Type V secretion system is present in all *Paraburkholderia* endophytes except *Ca.* Paraburkholderia dryadicola. The flagellar apparatus is missing in *Ca.* P. dryadicola, *Ca.* P. soutpansbergensis, and *P. phenoliruptrix* Vesc, and is incomplete in some other *P. phenoliruptrix* endophytes. Lastly, only the genomes of *Paraburkholderia caledonica* endophytes encode a complete set of core Type VI secretion system proteins.

Genes related to secondary metabolism are enriched in leaf endophytes

We wondered if specific metabolic pathways might be enriched in genomes of leaf symbionts, despite rampant reductive evolution. We assigned KEGG pathway membership for each predicted functional CDS (thus excluding predicted pseudogenes) in leaf symbiont genomes as well as a set of free-living representative *Paraburkholderia* or *Caballeronia* species. The number of genes assigned to a majority of the KEGG pathways (256 pathways in total) was significantly smaller in endophyte genomes compared to their free-living relatives.

A small portion (86 pathways) did not differ between leaf symbionts and free-living representatives. Genes belonging to a single pathway were significantly enriched in leaf endophytes: acarbose and validamycin biosynthesis (KEGG pathway map00525). Acarbose and validamycin are aminocyclitols synthesized via 2-*epi*-5-*epi*-valiolone synthase (EEVS). EEVS catalyses the first committed step of C_7N aminocyclitol synthesis[23,24], and likely plays a role in the production of kirkamide, a natural C_7N aminocyclitol present in leaves of *Psychotria kirkii* and other nodulated Rubiaceae, as well as streptol and streptol glucoside, 2 cyclitols with herbicidal activities (Pinto-Carbó *et al.*, 2016). Indeed, of 10 *Ca.* Burkholderia kirkii genes assigned to KEGG pathway map00525, 8 genes were previously hypothesised to play a direct role in the synthesis of C_7N aminocyclitol or derived compounds (Pinto-Carbó *et al.*, 2016). Similarly, 7 out of 11 orthogroups most enriched in leaf endophytes were linked to cyclitol synthesis (Table S7). To gain a better understanding of the distribution of cyclitol biosynthetic clusters in leaf endophytes, we searched for homologs of the two 2-*epi*-5-*epi*-valiolone synthase (EEVS) genes of *Ca.* Burkholderia kirkii (locus tags BKIR_C149_4878 and BKIR_C48_3593) in the other leaf endophyte genomes. We detected putative EEVS homologs in all but the two genomes of *Ca.* B. crenata. For *Ca.* B. crenata UZHbot9 we have previously shown the genome encodes a non-ribosomal peptide synthase likely responsible for the synthesis of the depsipeptide FR900359 (Fujioka *et al.*, 1988; Carlier *et al.*, 2016; Crüsemann *et al.*, 2018), and these genes were also detected in *Ca.* B. crenata Avir. Because EEVSs are phylogenetically related to 3-dehydroquinate synthases (DHQS), we aligned the putative EEVS sequences retrieved from leaf endophytes to EEVS and DHQS sequences in the Swissprot database. All putative EEVS sequences retrieved from leaf endophytic *Burkholderia* were phylogenetically related to *bona fide* EEVS proteins, but not to dehydroquinate synthase (DHQS) and other sedoheptulose 7-phosphate cyclases. EEVS are otherwise rare in *Burkholderia* s. l., with putative EEVSs present in only 11 out of 5674 publicly available *Burkhoderiaceae* genomes (excluding leaf symbiotic bacteria) in the NCBI RefSeq database as of June 2022 (Figure S7).

Evolution of cyclitol metabolism in leaf endophytic Burkholderia

Phylogenetic analysis of the endophyte EEVS protein sequences showed the presence of two main clades of *Burkholderia* EEVS homologs, as well as a divergent homolog in the genome of *Ca.* B. ardisicola Acor, and a second divergent homolog in *Ca.* P. dryadicola (Figure 2A).

The gene context of these EEVS genes in the different clades reveals that the two main EEVS clades correspond to the two conserved gene clusters previously hypothesized to play a role in kirkamide and streptol glucoside biosynthesis in *Ca.* Burkholderia kirkii (Carlier *et al.*, 2013). The gene order of these clusters is very similar in every genome, with a similar genomic context in closely related genomes (Table 2-3). These gene clusters are generally flanked by multiple mobile elements, consistent with acquisition via horizontal gene transfer. Furthermore, the EEVS phylogeny did not follow the species phylogeny, indicating that HGT or gene conversion occurred (Figure 2). For clarity, we named the two main putative cyclitol biosynthetic gene clusters S-cluster (for streptol) and K-cluster (for kirkamide) based on previous biosynthetic hypotheses from *in silico* analysis of the putative cyclitol gene clusters of *P. kirkii* (Figure 2) (Pinto-Carbó *et al.*, 2016). Both K and S-clusters encode a core set of proteins linked to sugar analog biosynthesis: a ROK family protein and a HAD family hydrolase, and both contain aminotransferases (although from different protein families). Two EEVS genes contain nonsense mutations and are likely not functional: the S-cluster EEVS of *Ca.* Burkholderia humilis, and the K-cluster EEVS of *Ca.* Burkholderia brachyanthoides. The genome of *Ca.* B. humilis still contains an apparently functional K-cluster EEVS, while the pseudogenized EEVS of *Ca.* B. brachyanthoides is the only homolog in the genome. Interestingly, genes of the K-cluster appear to be exclusive to *Psychotria* and *Pavetta* symbionts, while the S-cluster is more widespread, including in the genomes of *Vangueria* endophytes. Accordingly, we detected kirkamide in leaf extracts of *Psychotria kirkii*, but in none of the *Fadogia* or *Vangueria* species we tested (see supplementary methods). We also detected signals that were consistent with streptol/valienol and streptol glucoside by UPLC-QToF-MS in all samples. However, these signals occurred in a noisy part of the chromatogram, and we could not confidently assign these m/z features to streptol or its derivatives (see supplementary methods).

The genomes of *Ca.* P. soutpansbergensis and *P. caledonica* R-49542 and R-82532 encoded EEVS homologs of the K-cluster, but the full complement of the genes of the K-cluster is missing (Table 3). In both cases the EEVS gene is flanked by IS elements. Accordingly, we did not detect kirkamide in leaf samples from either *Fadogia homblei* or *P. soutpansbergensis* in our chemical analyses. The genome of *Ca.* P. dryadicola encodes an EEVS that clusters outside of the K- and S-EEVS clusters. Genes with putative functions similar to those of the K-

454 cluster are located in the vicinity of the EEVS in the genome of *Ca.* P. dryadicola:
455 oxidoreductases, an aminotransferase, and an N-acetyltransferase (Table S8). Similarly, *Ca.*
456 B. ardisicola Acor contains a second divergent EEVS, in addition to the S-cluster EEVS. This
457 EEVS belongs to a larger gene cluster coding for similar functions also found in the other
458 EEVS-clusters, but contains at least one frameshift mutation and no longer codes for a
459 functional enzyme (Table S8). Lastly, *Ca.* B. verschuerenii contains a second, recently
460 diverged EEVS paralog of the K-cluster. This EEVS is part of a small cluster of genes, with
461 putative functions divergent from those found in the other EEVS-clusters and likely does not
462 play a role in kirkamide synthesis (Table S8).

463

Discussion

Different evolutionary origins of leaf symbioses in different plant genera

In this work, we investigated the evolution of associations between *Burkholderia s. l.* bacteria and plants of the Rubiaceae and Primulaceae families, and attempted to identify key characteristics of these associations. To this end, we re-analyzed publicly available genome data from previous research, and sequenced and assembled the genomes of an additional 17 leaf endophytes. In addition to leaf endophytes which had been previously detected (Lemaire, Smets, *et al.*, 2011; Verstraete *et al.*, 2011, 2013; Ku and Hu, 2014), we document here the presence of *Burkholderia s.l.* symbionts in *Pavetta hochstetteri* and *Vangueria esculenta*, and possibly *Pavetta revoluta*. In contrast to previous findings (Lemaire, Lachenaud, *et al.*, 2012), we could not detect evidence of leaf endophytes in *Psychotria capensis*, but did confirm the absence of leaf endophytes in *Psychotria zombamontana*. Phylogenetic placement of hosts and endophytes are consistent with previous data, except for the placement of *Vangueria macrocalyx* and its endophyte (Lemaire, Lachenaud, *et al.*, 2012; Verstraete *et al.*, 2013). Both chloroplast sequences of *V. macrocalyx* and *V. dryadum* and the genomes of their endophytes were near identical while previous research showed a clear phylogenetic difference both between the host species and their endophytes (Verstraete *et al.*, 2013). Blastn analysis of plant genetic markers (ITS, petB, rpl16, trnTF) of both species against the NCBI nr database showed higher identities to markers from *Vangueria dryadum* than to those of *Vangueria macrocalyx*. However, since comparison of the vouchered *V. macrocalyx* specimen to other vouchered *Vangueria dryadum* and *V. macrocalyx* by expert botanists clearly separated both species, we decided to consider both species distinct.

Previous studies showed that Rubiaceae and Primulaceae species with heritable leaf symbionts are monophyletic within their respective genera (Lemaire, Vandamme, *et al.*, 2011; Verstraete *et al.*, 2013). Thus, while the transition to a symbiotic state arose separately in multiple plant genera, it likely evolved only once in each plant genus. The only exception is the *Psychotria* genus, where it likely arose twice: once in species forming leaf nodules, and once in species without leaf nodules (Lemaire, Lachenaud, *et al.*, 2012). The repeated emergence of leaf symbiosis is reflected on the microbial side as well. A parsimonious interpretation of whole genome phylogenetic analyses indicates that

Burkholderia endophytes evolved independently at least 8 times, most probably from ancestors with an environmental lifestyle (Figure 1A). *Caballeronia* endophytes of *Ardisia* seem to have emerged once, with most closely related species commonly isolated from soil (Lim *et al.*, 2003; Vandamme *et al.*, 2013; Uroz and Oger, 2017). As previously reported, symbionts of *Psychotria* and *Pavetta* cluster in 3 distinct phylogenetic groups within the *Caballeronia* genus. Finally, symbionts of *Vangueria* and *Fadogia* belong to 5 distinct clades within the genus *Paraburkholderia*. Apart from *Ca.* P. dryadicola that is without closely related isolates, endophytic *Paraburkholderia* species also cluster together with species commonly isolated from soil (Verstraete *et al.*, 2014; Beukes *et al.*, 2019). High host-specificity is a hallmark of the *Psychotria*, *Pavetta*, and *Ardisia* leaf symbiosis, but this characteristic is not shared in *Vangueria* and *Fadogia*. Based on genome similarity, we identified at least three phylogenetically divergent endophyte species that can infect multiple hosts: *P. caledonica*, *P. phenoliruptrix*, and *Ca.* P. dryadicola. It is also possible that these plants are in the early stages of endophyte capture, where the plant is open to acquire endophytes from the soil, as previously hypothesized for *F. homblei* (Verstraete *et al.*, 2013). Endophytes might later evolve to become host-restricted and vertically transmitted, leading to diversification from their close relatives and forming new species. This could, for example, already be the case for *Ca.* P. soutpansbergensis, which is related to *P. phenoliruptrix* but shows a more divergent genome (ANI <95%). Overall, these results highlight the general plasticity of bacteria in the *Burkholderia s.l.*, as well as the probable frequent occurrence of host-switching or horizontal transfer within leaf symbiotic associations.

Genome reduction is a common treat of leaf endophytes

Bacterial genomes contain a wealth of information yet few leaf endophyte genomes are available. In this study we provide an additional thirteen leaf endophyte genome assemblies among which the first genomes of endophytes from *Vangueria* and *Fadogia*. Aside from the genomes of *P. caledonica* endophytes, all leaf endophyte genomes were small, mostly between 3.5 and 5 Mbp. This is well below the average 6.85 Mbp of the *Burkholderiaceae* family (Carlier *et al.*, 2016; Pinto-Carbó *et al.*, 2016). In addition to their small sizes, the genomes of *Psychotria*, *Pavetta*, and *Ardisia* endophytes show signs of advanced genome reduction. Only 41-70% of these genomes code for functional proteins, compared to an average of about 90% for free-living bacteria (Land *et al.*, 2015). Most of these genomes also

contain a high proportion of mobile sequences, up to 9% of the total assembly. Together, this indicates ongoing reductive genome evolution, a process often observed in obligate endosymbiotic bacteria (Moran and Plague, 2004; Bennett and Moran, 2015). Interestingly, the genomes of *Vangueria* and *Fadogia* endophytes, which are not contained in leaf nodules, also show signs of genome erosion: most genomes of *P. phenoliruptrix* endophytes are at or below 5 Mbp in size, with over half of their proteome predicted as non-functional. The genomes of *Ca.* P. dryadicola even approach the level of genome reduction found in most *Psychotria* symbionts. The intermediate genome reduction in endophytes of *Vangueria* and *Fadogia* could be explained by the relatively recent origin of the symbiosis, although leaf symbiosis in *Fadogia* has been estimated to be older than in *Vangueria* (7.6 Mya vs. 3.7 Mya) (Verstraete *et al.*, 2017). Other factors likely contribute to the extent or pace of genome reduction in the endophytes, such as mode of transmission and transmission bottlenecks. The larger genome size and fewer pseudogenes compared to most other leaf endophytes may explain why we could isolate *P. caledonica* endophytes from *F. homblei*, but not other endophytes. We could not identify essential genes or pathways that were consistently missing in the genomes of *Burkholderia* endophytes. It is therefore possible that other endophytic bacteria may be culturable using more complex or tailored culture conditions.

Secondary metabolism as key factor in the evolution of leaf symbiosis

Although leaf symbionts share a similar habitat and all belong to the *Burkholderia s. l.*, their core genome is surprisingly small and consists almost entirely (95%) of genes that are considered essential for cellular life. This poor conservation of accessory functions perhaps reflects the large diversity and possible redundancy of functions encoded in the genomes of *Burkholderia s.l.* that associate with plants. Interestingly, the capacity for production of secondary metabolites is a key common trait of *Burkholderia* leaf endophytes. We previously showed that *Ca.* B. crenata produces FR900359, a cyclic depsipeptide isolated from *A. crenata* leaves (Carlier *et al.*, 2016). This non-ribosomal peptide possesses unique pharmacological properties and may contribute to the protection of the host plant against insects (Carlier *et al.*, 2016; Crüsemann *et al.*, 2018). However, our data suggests that the production of cyclitols is widespread in leaf endophytic *Burkholderia*. Indeed, with the exception of *Ca*. B. crenata cited above, we found evidence for the presence of cyclitol biosynthetic pathways in all genomes of leaf endophytic *Burkholderia*. We have previously

reported the presence of two gene clusters containing a 2-*epi*-5-*epi*-valiolone synthase (EEVS) in the genomes of *Psychotria* and *Pavetta* symbionts (Pinto-Carbó *et al.*, 2016). These gene clusters are likely responsible for the production of 2 distinct cyclitols: kirkamide, a C_7N aminocyclitol with insecticidal properties which has been detected in several *Psychotria* plants; and streptol-glucoside, a plant-growth inhibitor likewise detected in *Psychotria kirkii* (Sieber *et al.*, 2015; Pinto-Carbó *et al.*, 2016; Hsiao *et al.*, 2019). EEVS from leaf symbionts belong to four phylogenetic clusters, including the two EEVS genes previously detected in *Psychotria* and *Pavetta* symbionts (Pinto-Carbó *et al.*, 2016). Similar to these previously analysed leaf endophyte genomes, the EEVS gene clusters in the newly sequenced genomes are flanked by IS-elements, and their phylogeny is incongruent with the species phylogeny. This indicates that these genes and clusters are likely acquired via horizontal gene transfer. This hypothesis is strengthened by the fact that the closest homologs of the genes in the EEVS clusters are found in genera as diverse as *Pseudomonas*, *Streptomyces*, and *Noviherbaspirillum*, but are rare in the genomes of *Burkholderia s.l.* The presence of the two main EEVS gene clusters (K-cluster and S-cluster) is not strictly linked to the symbiont or host taxonomy. For example, the EEVS of the K-cluster (hypothesised to produce kirkamide) is present in all sequenced symbionts of *Psychotria* and *Pavetta* but also in the endophytes of *F. homblei* and *V. soutpansbergensis*. However, in the latter two, accessory genes of the K-cluster are absent. It is possible that this EEVS interacts with gene products of other secondary metabolite clusters (Osborn *et al.*, 2017). We also noticed that some endophyte genomes contain multiple EEVS genes or gene clusters. This could provide functional redundancy, protecting against the rampant genome erosion present in these genomes. For example, two genes of the S-cluster *Ca.* B. hochstetteri are likely pseudogenes, while the K-cluster gene is still complete. On the other hand, in *Ca.* Burkholderia humilis seven out of ten genes of the S-cluster (including the EEVS) are either missing or non-functional, and the K-cluster is heavily reduced with only four functional genes out of eight (including the EEVS). As one functional EEVS copy remains, it is possible that genes located elsewhere in the genome provide these functions, as kirkamide has previously been detected in extracts of *Psychotria humilis* (Pinto-Carbó *et al.*, 2016). Alternatively, this symbiosis may have reached a "point of no return" where host and symbiont have become dependent on each other and non-performing symbionts can become fixed in the population (Bennett and Moran, 2015).

588 The presence of gene clusters coding for specialised secondary metabolites in all leaf
589 symbionts could indicate that secondary metabolite production is either a prerequisite for or
590 a consequence of an endophytic lifestyle. The fact that *P. caledonica* leaf symbionts have
591 EEVS genes of different origin favours the hypothesis that the acquisition of secondary
592 metabolism precedes an endophytic lifestyle. In this case, the ancestor of both endophytes
593 may have acquired differing EEVS genes or EEVS gene clusters through HGT followed by
594 infection of the respective host plants. The lack of EEVS homolog in *Ca.* B. crenata indicates
595 that production of cyclitols is not essential for leaf symbiosis. Interestingly, genomes of the
596 sister species *Ca.* B. ardisicola encode an EEVS and the full S-cluster complement. Since there
597 is strong phylogenetic evidence of co-speciation in the *Burkholderia*/*Ardisia* association
598 (Lemaire, Smets, *et al.*, 2011; Ku and Hu, 2014), the common ancestor of *Ca*. B. ardisicola
599 and *Ca.* B. crenata possibly possessed both cyclitols and *frs* pathways, and one of these
600 pathways was lost in the lineages leading to contemporary *Ca*. B. crenata and *Ca*. B.
601 ardisicola. Alternatively, the genome of the common ancestor of *Ardisia*-associated
602 *Burkholderia* may have encoded cyclitol S-cluster and later acquisition of the *frs* gene cluster
603 in the Ca. B. crenata lineage alleviated the requirement of EEVS-related metabolism. The
604 model of horizontal acquisition of secondary functions supports the model of endophyte
605 evolution described by Lemaire *et al* (Lemaire, Vandamme, *et al.*, 2011). Different
606 environmental strains which acquired genes for secondary metabolite production could
607 colonise different host plants in the early open phase of symbiosis. The different
608 phylogenetic endophyte clades observed in the *Burkholderia s.l.* phylogeny could each
609 represent distinct acquisitions of secondary metabolite gene clusters by divergent free-living
610 bacteria followed by colonisation of different host plants. Many *Burkholderia* species
611 associate with eukaryotic hosts, including plants (Eberl and Vandamme, 2016), and many of
612 these associations may be transient in nature. However, useful traits such as synthesis of
613 protective metabolites may help stabilise these relationships, resulting in long-term
614 associations such as leaf symbiosis.

615 **Author contributions:**

616 AC, MM, and BD designed the research. MM identified and collected wild plant specimens
617 from the Pretoria region (South Africa). BD, MB, SS, and AC performed the laboratory

618 experiments and analyses. BD, MM and AC wrote the manuscript with input from all
619 authors.

620 **Acknowledgments**

621 We would like to thank Frédéric De Meyer and Mathijs Deprez for helping with some of the
622 laboratory experiments. We would further like to thank Steven Janssens (Meise Botanic
623 Garden) and Peter Brownless (Royal Botanic Garden Edinburgh) for facilitating the
624 acquisition of plant material for this study. BD and AC would like to thank Klaas Vandepoele,
625 Monica Höfte, Anne Willems and Paul Wilkin for helpful discussion and for proofreading the
626 manuscript. We also thank Aurélien Bailly (University of Zürich, CH) for providing *P. kirkii*
627 samples and help with interpreting mass spectrometry data. Magda Nel of the H.G.W.J.
628 Schweickerdt Herbarium is thanked for her help with plant identification and Mamoalosi
629 Selepe and Sewes Alberts of the Chemistry and Plant and Soil Sciences Departments,
630 respectively (University of Pretoria) for chemical analysis. We also thank Chien-Chi Hsiao and
631 Karl Gademann from University of Zürich (Switzerland) for providing the analytical standards.
632 This work was supported by the Flemish Fonds Wetenschappelijk Onderzoek under grant
633 G017717N to AC. AC also acknowledges support from the French National Research Agency
634 under grant agreement ANR-19-TERC-0004-01 and from the French Laboratory of Excellence
635 project "TULIP" (ANR-10-LABX-41; ANR-11-IDEX-0002-02) and from the French National
636 Infrastructure for Metabolomics and Fluxomics, Grant MetaboHUB-ANR-11-INBS-0010. We
637 thank the Oxford Genomics Centre at the Wellcome Centre for Human Genetics for the
638 collection and preliminary analysis of sequencing data. The Oxford Genomics Centre at the
639 Wellcome Centre for Human Genetics is funded by Wellcome Trust grant reference
640 203141/Z/16/Z. The funders had no role in study design, data collection and analysis,
641 decision to publish, or preparation of the manuscript.

642 **Notes**

643 The authors declare no conflict of interest.

644 *Figure Legends*

645 **Figure 1: Phylogeny of *Burkholderia, Caballeronia,* and *Paraburkholderia*, including the leaf endophytes. (A)**
646 UBCG phylogeny of the *Burkholderia* s.l. based on 92 conserved genes. Bootstrap support values based on 100
647 replications are displayed on the branches. Branches with <50% support were collapsed. *Ralstonia*
648 *solanacearum* was used as outgroup to root the tree. Coloured samples in boldface represent the leaf
649 endophytes from Rubiaceae and Primulaceae **(B)** Core genome phylogeny of leaf endophytes based on
650 alignment of 423 single-copy core genes. Bootstrap support values based on 100 replicates are shown on the
651 branches. Samples are colour-coded based on the host genus: Purple – *Ardisia*; Blue – *Psychotria*; Pink –
652 *Pavetta*; Green – *Vangueria*; Orange – *Fadogia*; Black bars represent the coding capacity of the genome (the
653 proportion of the genome coding for functional proteins).

654 **Figure 2: EEVS protein phylogeny and distribution in leaf endophytes. (A)** EEVS protein phylogeny of detected
655 EEVS-genes and their closest relatives. Local support values based on the Shimodaira-Hasegawa test are shown
656 on the branches, and branches with support <50% are collapsed. Coloured samples in boldface are the EEVS
657 homologs found in different leaf endophytes. Colours represent different clusters of similar EEVS genes. K- and
658 S-cluster are named after their putative products (K for Kirkamide, and S for Streptol glucoside). NCBI accession
659 numbers of the close relatives are given next to their species name. The tree is rooted using related 3-
660 dehydroquinate synthase genes (not shown). *The EEVS gene in *Ca*. Burkholderia humilis contains an internal
661 stop codon, creating two EEVS-like pseudogenes. The largest of both was used for the phylogeny. **This EEVS
662 gene of *Ca.* Burkholderia verschuerenii is found outside of the K-cluster. **(B)** Distribution of specialised
663 metabolism in the leaf endophytes. Samples are colour-coded based on the host species: Purple – *Ardisia*; Blue
664 – *Psychotria*; Pink – *Pavetta*; Green – *Vangueria*; Orange – *Fadogia*. Codes next to the species represent
665 presence of specialised metabolite clusters; FR – FR900359 depsipeptide; K – Kirkamide EEVS-cluster; S –
666 Streptol glucoside EEVS-cluster; O – Other EEVS-cluster. K' – Secondary EEVS cluster with EEVS similar to the K-
667 cluster. K* - Only the K-cluster EEVS is present, not the accessory genes.

Tables

Table 1: Genome statistics of newly assembled and re-assembled leaf endophyte genomes. Coding capacity refers to the proportion of the genome that codes for functional proteins.

Endophyte	Host species	Type	Assembly size (Mb)	Contigs	N50 (bp)	%G+C	Annotated genes	Functional genes	Pseudo genes	Coding Capacity (%)	IS elements	IS total length (bp)	Proportion IS (%)
Ca. **Burkholderia ardisicola Acor**	*Ardisia cornudentata*	New assembly	3,95	332	19528	59,23	6975	2026	4949	40,30	35	32834	0,83
Ca. **Burkholderia crenata UZHbot9**	*Ardisia crenata*	Re-assembly	2,65	607	6399	59,02	3982	1670	2312	54,73	96	69678	2,63
Ca. **Burkholderia ardisicola Amam**	*Ardisia mamillata*	New assembly	4,38	333	19687	59,47	7472	2297	5175	40,95	59	48385	1,10
Ca. **Burkholderia crenata Avir**	*Ardisia virens*	New assembly	2,58	605	6517	59,05	3839	1648	2191	56,13	63	42190	1,64
Paraburkholderia caledonica **R-49542**	*Fadogia homblei*	New assembly	8,92	148	145314	61,59	9185	7695	1490	82,83	96	117852	1,32
Paraburkholderia caledonica **R-82532**	*Fadogia homblei*	New assembly	8,71	123	239289	61,53	9054	7353	1701	81,03	77	91097	1,05
Ca. **Burkholderia hochstetteri**	*Pavetta hochstetteri*	New assembly	3,50	324	18152	62,51	5453	1823	3630	44,53	29	38062	1,09
Ca. **Burkholderia schumanniana**	*Pavetta schumanniana*	Re-assembly	3,62	412	14848	63,47	4938	2453	2485	59,95	69	44239	1,22
Ca. **Burkholderia brachyanthoides**	*Psychotria brachyanthoides*	Re-assembly	3,75	648	8356	61,00	6284	2109	4175	46,54	223	149135	3,98
Ca. **Burkholderia humilis**	*Psychotria humilis*	Re-assembly	5,32	238	103328	59,60	7828	3264	4564	50,04	64	63278	1,19
Ca. **Burkholderia kirkii**	*Psychotria kirkii*	Reference	4,01	203	44916	62,91	6329	2069	4260	45,80	375	353298	8,81
Ca. **Burkholderia pumila**	*Psychotria pumila*	Re-assembly	3,70	463	12628	59,13	6835	2192	4643	45,41	195	153499	4,15
Ca. **Burkholderia punctata**	*Psychotria punctata*	Reference	3,91	48	100248	64,00	4864	2539	2325	54,61	310	358729	9,17
Ca. **Burkholderia umbellata**	*Psychotria umbellata*	Re-assembly	4,22	333	28025	61,30	6967	2306	4661	44,37	91	68761	1,63
Ca. **Burkholderia verschuerenii**	*Psychotria verschuerenii*	Re-assembly	6,15	401	27267	62,07	7440	4839	2601	70,21	88	60714	0,99
Ca. **Paraburkholderia dryadicola Vdry**	*Vangueria dryadum*	New assembly	4,29	153	50748	61,26	7076	2229	4847	43,21	38	35272	0,82
Paraburkholderia phenoliruptrix **Vesc**	*Vangueria esculenta*	New assembly	4,99	180	50333	63,54	6347	3329	3018	59,78	46	54597	1,09
Paraburkholderia phenoliruptrix **Vinf**	*Vangueria infausta*	New assembly	5,00	181	49920	63,51	6377	3320	3057	59,29	50	58387	1,17
Ca. **Paraburkholderia dryadicola Vmac**	*Vangueria macrocalyx*	New assembly	4,31	150	54987	61,30	7111	2243	4868	43,06	40	37709	0,87

***Paraburkholderia phenoliruptrix* VmadMBG**	*Vangueria madagascariensis*	New assembly	4,77	247	34361	63,48	5912	3214	2698	61,09	45	55093	1,15
***Paraburkholderia phenoliruptrix* VmadEBG**	*Vangueria madagascariensis*	New assembly	4,76	242	34985	63,48	5901	3212	2689	60,97	45	53173	1,12
***Paraburkholderia phenoliruptrix* VmadSA**	*Vangueria madagascariensis*	New assembly	5,03	194	50250	63,49	6444	3291	3153	59,22	47	48936	0,97
***Paraburkholderia caledonica* Vpyg88**	*Vangueria pygmaea*	New assembly	7,44	92	232014	61,89	7426	6194	1232	82,23	54	74083	1,00
***Paraburkholderia caledonica* Vpyg08**	*Vangueria pygmaea*	New assembly	7,45	106	232088	61,90	7449	6193	1256	82,33	60	79510	1,07
***Paraburkholderia phenoliruptrix* Vran**	*Vangueria randii*	New assembly	4,98	205	50270	63,33	6379	3294	3085	59,47	59	73129	1,47
***Ca.* Paraburkholderia soutpansbergensis**	*Vangueria soutpansbergensis*	New assembly	5,18	51	337347	63,12	6801	3259	3542	55,24	35	44578	0,86

Table 2: EEVS S-cluster organisation in endophyte genomes. Genomes of the same host with the same cluster layout are merged. X: Gene present; -: Gene absent; **Ψ**: Gene predicted to be pseudogene; *: genes present on a different contig than the EEVS gene; Abbreviations: EEVS – 2-*epi*-5-*epi*-valiolone synthase;

	ROK family protein	EEVS	Sugar-nucleotide binding protein	Trehalose-6-phosphate synthase	Aspartate aminotransferase family protein	Alcohol dehydrogenase	HAD family hydrolase	MFS transporter	NTP-transferase	NUDIX hydrolase
Reference accessions	CCD39391	CCD39393	CCD39394	CCD39395	KND54529	CCD39396	CCD39397	CCD39398	CCD39400	CCD39401
Ca. Burkholderia ardisicola Acor	X	X	X	X	X	X	X	X	X	X
Ca. Burkholderia ardisicola Amam	X	X	X	X	X	X	X	X	X	X
Ca. Burkholderia *hochstetteri*	X	X	X	**Ψ**	**Ψ**	X	X	X	X	X
Ca. Burkholderia humilis	X	**Ψ**	X	**Ψ**	X	-	-	-	-	**Ψ**
Ca. Burkholderia kirkii	X	X	X	X	-	X	X	X	**Ψ**	X
Ca. Burkholderia punctata	X	X	X	X	X	X	X	X	X	-
Ca. Burkholderia schumanniana	X	X	X	X	X	X	-	**Ψ***	X*	X*
Paraburkholderia phenoliruptrix Vesc	X	X	X	X	X	X	X	X	X	**Ψ**
Paraburkholderia phenoliruptrix Vinf	X	X	X	X	X	X	**Ψ**	X	X	**Ψ**
Paraburkholderia phenoliruptrix VmadSA	X	X	X	X	X	X	X	X	X	**Ψ**
Paraburkholderia phenoliruptrix VmadMBG/VmadBGE	X	X	X	X	X	X	**Ψ**	X	X	**Ψ**
Paraburkholderia caledonica Vpyg08/Vpyg88	X	X	X	X	X	X	X	X	X	X
Paraburkholderia phenoliruptrix Vran	X	X	X	X	X	X	X	X	X	X

Table 3: EEVS K-cluster organisation in endophyte genomes. Genomes of the same host with the same cluster layout are merged. X: Gene present; -: Gene absent; **Ψ**: Gene predicted to be pseudogene; *: protein overlaps with contig end, other genes of the cluster not found on other contigs; Abbreviations: EEVS – 2-*epi*-5-*epi*-valiolone synthase.

	GNAT family N-acetyltransferase	Cupin Domain Containing protein	HAD family hydrolase	Gfo/Idh/MocA family oxidoreductase	6-phospho-beta-glucosidase	DegT/DnrJ/EryC1/StrS family aminotransferase	ROK family protein	EEVS
Reference accessions	CCD36711	CCD36712	CCD36713	CCD36714	CCD36715	CCD36716	CCD6717	CCD36718
***Paraburkholderia caledonica* R-49542/R-82532**	-	-	-	-	-	-	-	X
***Ca.* Burkholderia brachyanthoides**	-	-	-	-	-	-	X/Ψ *	**Ψ**
***Ca.* Burkholderia hochstetteri**	X	X	X	X	X	X	X	X
***Ca.* Burkholderia humilis**	-	X	**Ψ**	X	X	**Ψ**	X	X
***Ca.* Burkholderia kirkii**	X	X	X	X	X	X	X	X
***Ca.* Burkholderia pumila**	-	X	X	X	X	X	X	X
***Ca.* Burkholderia punctata**	X	X	X	X	X	X	X	X
***Ca.* Burkholderia schumanniana**	X	X	X	X	X	X	X	X
***Ca.* Burkholderia umbellata**	X	X	X	X	X	X	X	X
***Ca.* Burkholderia verschuerenii**	X	X	X	X	X	X	X	X
***Ca.* Paraburkholderia soutpansbergensis**	-	-	-	-	-	-	-	X

References

Abby, S.S., Cury, J., Guglielmini, J., Néron, B., Touchon, M., and Rocha, E.P.C. (2016) Identification of protein secretion systems in bacterial genomes. *Sci Rep* **6**: 23080.

Abby, S.S., Néron, B., Ménager, H., Touchon, M., and Rocha, E.P.C. (2014) MacSyFinder: A Program to Mine Genomes for Molecular Systems with an Application to CRISPR-Cas Systems. *PLoS One* **9**: e110726.

Bankevich, A., Nurk, S., Antipov, D., Gurevich, A.A., Dvorkin, M., Kulikov, A.S., et al. (2012) SPAdes: A new genome assembly algorithm and its applications to single-cell sequencing. *J Comput Biol* **19**: 455–477.

Bennett, G.M. and Moran, N.A. (2015) Heritable symbiosis: The advantages and perils of an evolutionary rabbit hole. *Proc Natl Acad Sci U S A* **112**: 10169–76.

Bertels, F., Silander, O.K., Pachkov, M., Rainey, P.B., and van Nimwegen, E. (2014) Automated reconstruction of whole-genome phylogenies from short-sequence reads. *Mol Biol Evol* **31**: 1077–88.

Beukes, C.W., Steenkamp, E.T., van Zyl, E., Avontuur, J., Chan, W.Y., Hassen, A.I., et al. (2019) Paraburkholderia strydomiana sp. nov. and Paraburkholderia steynii sp. nov.: rhizobial symbionts of the fynbos legume Hypocalyptus sophoroides. *Antonie Van Leeuwenhoek* **112**: 1369–1385.

Brader, G., Compant, S., Vescio, K., Mitter, B., Trognitz, F., Ma, L.-J., and Sessitsch, A. (2017) Ecology and Genomic Insights into Plant-Pathogenic and Plant-Nonpathogenic Endophytes. *Annu Rev Phytopathol* **55**: 61–83.

Brettin, T., Davis, J.J., Disz, T., Edwards, R.A., Gerdes, S., Olsen, G.J., et al. (2015) RASTtk: A modular and extensible implementation of the RAST algorithm for building custom annotation pipelines and annotating batches of genomes. *Sci Rep* **5**: 8365.

Brundrett, M. (1991) Mycorrhizas in Natural Ecosystems. In *Advances in Ecological Research*. pp. 171–313.

Buchfink, B., Reuter, K., and Drost, H.-G. (2021) Sensitive protein alignments at tree-of-life scale using DIAMOND. *Nat Methods* **18**: 366–368.

Camacho, C., Coulouris, G., Avagyan, V., Ma, N., Papadopoulos, J., Bealer, K., and Madden, T.L. (2009) BLAST+: architecture and applications. *BMC Bioinformatics* **10**: 421.

Cantalapiedra, C.P., Hernández-Plaza, A., Letunic, I., Bork, P., and Huerta-Cepas, J. (2021) eggNOG-mapper v2: Functional Annotation, Orthology Assignments, and Domain Prediction at the Metagenomic Scale. *bioRxiv* 2021.06.03.446934.

Carlier, A. and Eberl, L. (2012) The eroded genome of a Psychotria leaf symbiont: Hypotheses about lifestyle and interactions with its plant host. *Environ Microbiol* **14**: 2757–2769.

Carlier, A., Fehr, L., Pinto-Carbó, M., Schäberle, T., Reher, R., Dessein, S., et al. (2016) The genome analysis of C andidatus Burkholderia crenata reveals that secondary metabolism may be a key function of the Ardisia crenata leaf nodule symbiosis. *Environ Microbiol* **18**: 2507–2522.

Carlier, A.L., Omasits, U., Ahrens, C.H., and Eberl, L. (2013) Proteomics analysis of Psychotria leaf nodule symbiosis: improved genome annotation and metabolic predictions. *Mol Plant Microbe Interact* **26**: 1325–33.

Carver, T., Harris, S.R., Berriman, M., Parkhill, J., and McQuillan, J.A. (2012) Artemis: an integrated platform for visualization and analysis of high-throughput sequence-based experimental data. *Bioinformatics* **28**: 464–469.

Chen, S., Zhou, Y., Chen, Y., and Gu, J. (2018) fastp: an ultra-fast all-in-one FASTQ preprocessor. *Bioinformatics* **34**: i884–i890.

Crüsemann, M., Reher, R., Schamari, I., Brachmann, A.O., Ohbayashi, T., Kuschak, M., et al. (2018) Heterologous Expression, Biosynthetic Studies, and Ecological Function of the Selective Gq-Signaling Inhibitor FR900359. *Angew Chemie Int Ed* **57**: 836–840.

Dangl, J.L. and Jones, J.D.G. (2001) Plant pathogens and integrated defence responses to infection. *Nature* **411**: 826–833.

Eberl, L. and Vandamme, P. (2016) Members of the genus Burkholderia: good and bad guys. *F1000Research* **5**: 1007.

Edwards, U., Rogall, T., Blöcker, H., Emde, M., and Böttger, E.C. (1989) Isolation and direct complete nucleotide determination of entire genes. Characterization of a gene coding for 16S ribosomal RNA. *Nucleic Acids Res* **17**: 7843–7853.

Emms, D.M. and Kelly, S. (2019) OrthoFinder: Phylogenetic orthology inference for comparative genomics. *Genome Biol* **20**: 238.

Fisher, R.M., Henry, L.M., Cornwallis, C.K., Kiers, E.T., and West, S.A. (2017) The evolution of host-symbiont dependence. *Nat Commun* **8**: 15973.

Fujioka, M., Koda, S., Morimoto, Y., and Biemann, K. (1988) Structure of FR900359, a cyclic depsipeptide from Ardisia crenata sims. *J Org Chem* **53**: 2820–2825.

Gaspar, J.M. (2018) NGmerge: merging paired-end reads via novel empirically-derived models of sequencing errors. *BMC Bioinformatics* **19**: 536.

Georgiou, A., Sieber, S., Hsiao, C.C., Grayfer, T., Gorenflos López, J.L., Gademann, K., et al. (2021) Leaf nodule endosymbiotic Burkholderia confer targeted allelopathy to their Psychotria hosts. *Sci Rep* **11**: 1–15.

Guindon, S., Dufayard, J.-F., Lefort, V., Anisimova, M., Hordijk, W., and Gascuel, O. (2010) New algorithms and methods to estimate maximum-likelihood phylogenies: assessing the performance of PhyML 3.0. *Syst Biol* **59**: 307–21.

Gundel, P.E., Rudgers, J.A., and Whitney, K.D. (2017) Vertically transmitted symbionts as mechanisms of transgenerational effects. *Am J Bot* **104**: 787–792.

Gurevich, A., Saveliev, V., Vyahhi, N., and Tesler, G. (2013) QUAST: quality assessment tool for genome assemblies. *Bioinformatics* **29**: 1072–1075.

Heberle, H., Meirelles, G.V., da Silva, F.R., Telles, G.P., and Minghim, R. (2015) InteractiVenn: a web-based tool for the analysis of sets through Venn diagrams. *BMC Bioinformatics* **16**: 169.

Hsiao, C.-C., Sieber, S., Georgiou, A., Bailly, A., Emmanouilidou, D., Carlier, A., et al. (2019) Synthesis and Biological Evaluation of the Novel Growth Inhibitor Streptol Glucoside, Isolated from an Obligate Plant Symbiont. *Chem - A Eur J* **25**: 1722–1726.

Huerta-Cepas, J., Szklarczyk, D., Heller, D., Hernández-Plaza, A., Forslund, S.K., Cook, H., et al. (2019) eggNOG 5.0: a hierarchical, functionally and phylogenetically annotated orthology resource based on 5090 organisms and 2502 viruses. *Nucleic Acids Res* **47**: D309–D314.

Inglis, P.W., Pappas, M. de C.R., Resende, L. V., and Grattapaglia, D. (2018) Fast and inexpensive protocols for consistent extraction of high quality DNA and RNA from challenging plant and fungal samples for high-throughput SNP genotyping and sequencing applications. *PLoS One* **13**: e0206085.

Ku, C. and Hu, J.-M.M. (2014) Phylogenetic and Cophylogenetic Analyses of the Leaf-Nodule Symbiosis in Ardisia Subgenus Crispardisia (Myrsinaceae): Evidence from Nuclear and Chloroplast Markers and Bacterial rrn Operons. *Int J Plant Sci* **175**: 92–109.

Land, M., Hauser, L., Jun, S.R., Nookaew, I., Leuze, M.R., Ahn, T.H., et al. (2015) Insights from 20 years of bacterial genome sequencing. *Funct Integr Genomics* **15**: 141–161.

Lemaire, B., Lachenaud, O., Persson, C., Smets, E., and Dessein, S. (2012) Screening for leaf-associated endophytes in the genus Psychotria (Rubiaceae). *FEMS Microbiol Ecol* **81**: 364–372.

Lemaire, B., Van Oevelen, S., De Block, P., Verstraete, B., Smets, E., Prinsen, E., and Dessein, S. (2012) Identification of the bacterial endosymbionts in leaf nodules of Pavetta (Rubiaceae). *Int J Syst Evol Microbiol* **62**: 202–209.

Lemaire, B., Robbrecht, E., van Wyk, B., Van Oevelen, S., Verstraete, B., Prinsen, E., et al. (2011) Identification, origin, and evolution of leaf nodulating symbionts of Sericanthe (Rubiaceae). *J Microbiol* **49**: 935–941.

Lemaire, B., Smets, E., and Dessein, S. (2011) Bacterial leaf symbiosis in Ardisia (Myrsinoideae, Primulaceae): molecular evidence for host specificity. *Res Microbiol* **162**: 528–534.

Lemaire, B., Vandamme, P., Merckx, V., Smets, E., and Dessein, S. (2011) Bacterial Leaf Symbiosis in Angiosperms: Host Specificity without Co-Speciation. *PLoS One* **6**: e24430.

Letunic, I. and Bork, P. (2019) Interactive Tree Of Life (iTOL) v4: recent updates and new developments. *Nucleic Acids Res* **47**: W256–W259.

Li, H., Handsaker, B., Wysoker, A., Fennell, T., Ruan, J., Homer, N., et al. (2009) The Sequence Alignment/Map format and SAMtools. *Bioinformatics* **25**: 2078–2079.

Lim, Y.W., Baik, K.S., Han, S.K., Kim, S.B., and Bae, K.S. (2003) Burkholderia sordidicola sp. nov., isolated from the white-rot fungus Phanerochaete sordida. *Int J Syst Evol Microbiol* **53**: 1631–1636.

Lo, W.S., Huang, Y.Y., and Kuo, C.H. (2016) Winding paths to simplicity: Genome evolution in facultative insect symbionts. *FEMS Microbiol Rev* **40**: 855–874.

Lòpez-Fernàndez, S., Sonego, P., Moretto, M., Pancher, M., Engelen, K., Pertot, I., and Campisano, A. (2015) Whole-genome comparative analysis of virulence genes unveils similarities and differences between endophytes and other symbiotic bacteria. *Front Microbiol* **6**: 419.

Mahmud, T. (2009) Progress in aminocyclitol biosynthesis. *Curr Opin Chem Biol* **13**: 161–170.

Mahmud, T. (2003) The C7N aminocyclitol family of natural products. *Nat Prod Rep* **20**: 137–166.

Manzano-Marín, A., Coeur d'acier, A., Clamens, A.-L., Orvain, C., Cruaud, C., Barbe, V., and Jousselin, E. (2018) A Freeloader? The Highly Eroded Yet Large Genome of the Serratia symbiotica Symbiont of Cinara strobi. *Genome Biol Evol* **10**: 2178–2189.

Manzano-Marín, A. and Latorre, A. (2016) Snapshots of a shrinking partner: Genome reduction in Serratia symbiotica. *Sci Rep* **6**: 32590.

Marçais, G., Delcher, A.L., Phillippy, A.M., Coston, R., Salzberg, S.L., and Zimin, A. (2018) MUMmer4: A fast and versatile genome alignment system. *PLOS Comput Biol* **14**: e1005944.

McCann, H.C. (2020) Skirmish or war: the emergence of agricultural plant pathogens. *Curr Opin Plant Biol* **56**: 147–152.

McCutcheon, J.P. and Moran, N.A. (2012) Extreme genome reduction in symbiotic bacteria. *Nat Rev Microbiol* **10**: 13–26.

Meier-Kolthoff, J.P. and Göker, M. (2019) TYGS is an automated high-throughput platform for state-of-the-art genome-based taxonomy. *Nat Commun* **10**: 2182.

Miller, I.J., Rees, E.R., Ross, J., Miller, I., Baxa, J., Lopera, J., et al. (2019) Autometa: automated extraction of microbial genomes from individual shotgun metagenomes. *Nucleic Acids Res* **47**: e57–e57.

Miller, I.M. (1990) Bacterial Leaf Nodule Symbiosis. *Adv Bot Res* **17**: 163–234.

Miller, I.M. and Donnelly, A.E. (1987) Location and distribution of symbiotic bacteria during floral development in Ardisia crispa. *Plant, Cell Environ* **10**: 715–724.

Mira, A., Ochman, H., and Moran, N.A.N.A. (2001) Deletional bias and the evolution of bacterial genomes. *Trends Genet* **17**: 589–596.

Moran, N.A., McCutcheon, J.P., and Nakabachi, A. (2008) Genomics and Evolution of Heritable Bacterial Symbionts. *Annu Rev Genet* **42**: 165–190.

Moran, N.A. and Plague, G.R. (2004) Genomic changes following host restriction in bacteria. *Curr Opin Genet Dev* **14**: 627–33.

Na, S.I., Kim, Y.O., Yoon, S.H., Ha, S. min, Baek, I., and Chun, J. (2018) UBCG: Up-to-date bacterial core gene set and pipeline for phylogenomic tree reconstruction. *J Microbiol* **56**: 281–285.

Nurk, S., Meleshko, D., Korobeynikov, A., and Pevzner, P.A. (2017) metaSPAdes: a new versatile metagenomic assembler. *Genome Res* **27**: 824–834.

Van Oevelen, S., De Wachter, R., Vandamme, P., Robbrecht, E., and Prinsen, E. (2002) Identification of the bacterial endosymbionts in leaf galls of Psychotria (Rubiaceae, angiosperms) and proposal of "Candidatus Burkholderia kirkii" sp. nov. *Int J Syst Evol Microbiol* **52**: 2023–2027.

Ondov, B.D., Bergman, N.H., and Phillippy, A.M. (2011) Interactive metagenomic visualization in a Web browser. *BMC Bioinformatics* **12**: 385.

Osborn, A.R., Almabruk, K.H., Holzwarth, G., Asamizu, S., LaDu, J., Kean, K.M., et al. (2015) De novo synthesis of a sunscreen compound in vertebrates. *Elife* **4**:.

Osborn, A.R., Kean, K.M., Alseud, K.M., Almabruk, K.H., Asamizu, S., Lee, J.A., et al. (2017) Evolution and Distribution of C 7 –Cyclitol Synthases in Prokaryotes and Eukaryotes. *ACS Chem Biol* **12**: 979–988.

Pearson, W.R. (2000) Flexible Sequence Similarity Searching with the FASTA3 Program Package. In *Bioinformatics Methods and Protocols*. New Jersey: Humana Press, pp. 185–219.

Pettersson, M.E. and Berg, O.G. (2007) Muller's ratchet in symbiont populations. *Genetica* **130**: 199–211.

Pinto-Carbó, M., Sieber, S., Dessein, S., Wicker, T., Verstraete, B., Gademann, K., et al. (2016) Evidence of horizontal gene transfer between obligate leaf nodule symbionts. *ISME J* **10**: 2092–105.

Ponsting, H. and Ning, Z. (2010) SMALT - A New Mapper for DNA Sequencing Reads. *F1000Posters* **1**: 1.

Price, M.N., Dehal, P.S., and Arkin, A.P. (2009) FastTree: computing large minimum evolution trees with profiles instead of a distance matrix. *Mol Biol Evol* **26**: 1641–50.

Prjibelski, A., Antipov, D., Meleshko, D., Lapidus, A., and Korobeynikov, A. (2020) Using SPAdes De Novo Assembler. *Curr Protoc Bioinforma* **70**:.

van Rhijn, P. and Vanderleyden, J. (1995) The Rhizobium-plant symbiosis. *Microbiol Rev* **59**: 124–142.

Richter, M., Rosselló-Móra, R., Oliver Glöckner, F., and Peplies, J. (2016) JSpeciesWS: a web server for prokaryotic species circumscription based on pairwise genome comparison. *Bioinformatics* **32**: 929–931.

Schneider, M., Tognolli, M., and Bairoch, A. (2004) The Swiss-Prot protein knowledgebase and ExPASy: providing the plant community with high quality proteomic data and tools. *Plant Physiol Biochem* **42**: 1013–1021.

Shigenobu, S., Watanabe, H., Hattori, M., Sakaki, Y., and Ishikawa, H. (2000) Genome sequence of the endocellular bacterial symbiont of aphids Buchnera sp. APS. *Nature* **407**: 81–86.

Sieber, S., Carlier, A., Neuburger, M., Grabenweger, G., Eberl, L., and Gademann, K. (2015) Isolation and Total Synthesis of Kirkamide, an Aminocyclitol from an Obligate Leaf Nodule Symbiont. *Angew Chemie Int Ed* **54**: 7968–7970.

Sinnesael, A., Eeckhout, S., Janssens, S.B., Smets, E., Panis, B., Leroux, O., and Verstraete, B. (2018) Detection of Burkholderia in the seeds of Psychotria punctata (Rubiaceae) – Microscopic evidence for vertical transmission in the leaf nodule symbiosis. *PLoS One* **13**: e0209091.

Smith, S.E. and Read, D.J. (2008) Mycorrhizal Symbiosis, Academic Press.

Souvorov, A., Agarwala, R., and Lipman, D.J. (2018) SKESA: strategic k-mer extension for scrupulous assemblies. *Genome Biol* **19**: 153.

Stamatakis, A. (2014) RAxML version 8: A tool for phylogenetic analysis and post-analysis of large phylogenies. *Bioinformatics* **30**: 1312–1313.

Toh, H., Weiss, B.L., Perkin, S.A.H., Yamashita, A., Oshima, K., Hattori, M., and Aksoy, S. (2006) Massive genome

erosion and functional adaptations provide insights into the symbiotic lifestyle of Sodalis glossinidius in the tsetse host. *Genome Res* **16**: 149–156.

Di Tommaso, P., Moretti, S., Xenarios, I., Orobitg, M., Montanyola, A., Chang, J.M., et al. (2011) T-Coffee: A web server for the multiple sequence alignment of protein and RNA sequences using structural information and homology extension. *Nucleic Acids Res* **39**: W13-7.

Uroz, S. and Oger, P. (2017) Caballeronia mineralivorans sp. nov., isolated from oak-Scleroderma citrinum mycorrhizosphere. *Syst Appl Microbiol* **40**: 345–351.

Vandamme, P., De Brandt, E., Houf, K., Salles, J.F., van Elsas, J.D., Spilker, T., and LiPuma, J.J. (2013) Burkholderia humi sp. nov., Burkholderia choica sp. nov., Burkholderia telluris sp. nov., Burkholderia terrestris sp. nov. and Burkholderia udeis sp. nov.: Burkholderia glathei-like bacteria from soil and rhizosphere soil. *Int J Syst Evol Microbiol* **63**: 4707–4718.

Vandamme, P., Peeters, C., De Smet, B., Price, E.P., Sarovich, D.S., Henry, D.A., et al. (2017) Comparative Genomics of Burkholderia singularis sp. nov., a Low G+C Content, Free-Living Bacterium That Defies Taxonomic Dissection of the Genus Burkholderia. *Front Microbiol* **8**: 1679.

Verstraete, B., Van Elst, D., Steyn, H., Van Wyk, B., Lemaire, B., Smets, E., and Dessein, S. (2011) Endophytic Bacteria in Toxic South African Plants: Identification, Phylogeny and Possible Involvement in Gousiekte. *PLoS One* **6**: e19265.

Verstraete, B., Janssens, S., and Rønsted, N. (2017) Non-nodulated bacterial leaf symbiosis promotes the evolutionary success of its host plants in the coffee family (Rubiaceae). *Mol Phylogenet Evol* **113**: 161–168.

Verstraete, B., Janssens, S., Smets, E., and Dessein, S. (2013) Symbiotic ß-Proteobacteria beyond Legumes: Burkholderia in Rubiaceae. *PLoS One* **8**: e55260.

Verstraete, B., Peeters, C., van Wyk, B., Smets, E., Dessein, S., and Vandamme, P. (2014) Intraspecific variation in Burkholderia caledonica: Europe vs. Africa and soil vs. endophytic isolates. *Syst Appl Microbiol* **37**: 194–9.

Vessey, J.K., Pawlowski, K., and Bergman, B. (2005) Root-based N2-fixing Symbioses: Legumes, Actinorhizal Plants, Parasponia sp. and Cycads. *Plant Soil* **274**: 51–78.

Wilson, K. (2001) Preparation of Genomic <scp>DNA</scp> from Bacteria. *Curr Protoc Mol Biol* **56**: 2.4.1-2.4.5.

Wood, D.E., Lu, J., and Langmead, B. (2019) Improved metagenomic analysis with Kraken 2. *Genome Biol* **20**: 257.

Wu, X., Flatt, P.M., Schlörke, O., Zeeck, A., Dairi, T., and Mahmud, T. (2007) A Comparative Analysis of the Sugar Phosphate Cyclase Superfamily Involved in Primary and Secondary Metabolism. *ChemBioChem* **8**: 239–248.

Xie, Z. and Tang, H. (2017) ISEScan: automated identification of insertion sequence elements in prokaryotic genomes. *Bioinformatics* **33**: 3340–3347.

Zhang, R. (2004) DEG: a database of essential genes. *Nucleic Acids Res* **32**: 271D – 272.

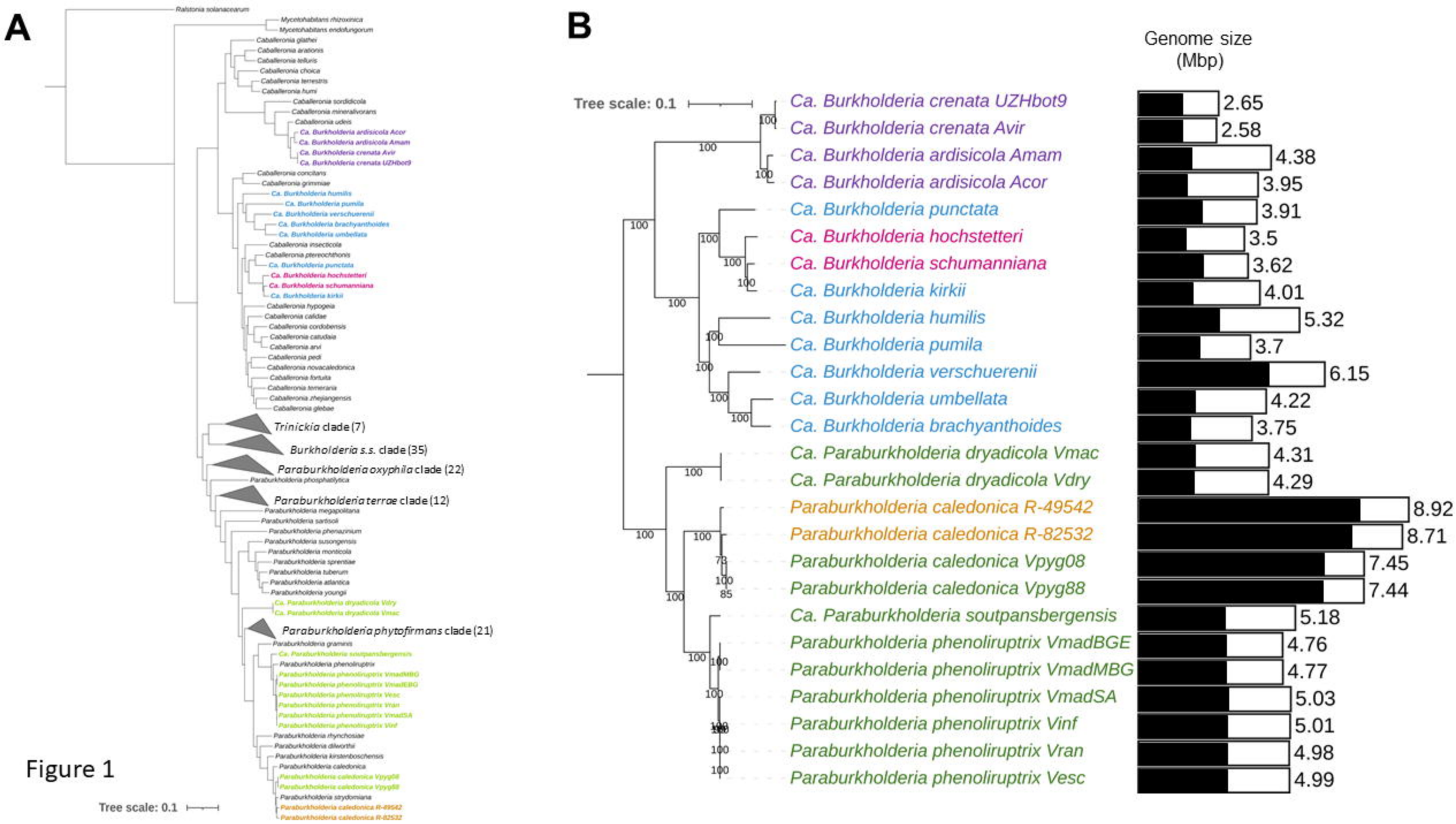
A
Ralstonia solanacearum
Mycetohabitans rhizoxinica
Mycetohabitans endofungorum
Caballeronia glathei
Caballeronia arationis
Caballeronia telluris
Caballeronia choica
Caballeronia terrestris
Caballeronia humi
Caballeronia sordidicola
Caballeronia mineralivorans
Caballeronia udeis
Ca. Burkholderia ardisicola Acor
Ca. Burkholderia ardisicola Amam
Ca. Burkholderia crenata Avir
Ca. Burkholderia crenata UZHbot9
Caballeronia concitans
Caballeronia grimmiae
Ca. Burkholderia humilis
Ca. Burkholderia pumila
Ca. Burkholderia verschuerenii
Ca. Burkholderia brachyanthoides
Ca. Burkholderia umbellata
Caballeronia insecticola
Caballeronia ptereochthonis
Ca. Burkholderia punctata
Ca. Burkholderia hochstetteri
Ca. Burkholderia schumanniana
Ca. Burkholderia kirkii
Caballeronia hypogeia
Caballeronia calidae
Caballeronia cordobensis
Caballeronia catudaia
Caballeronia arvi
Caballeronia pedi
Caballeronia novacaledonica
Caballeronia fortuita
Caballeronia temeraria
Caballeronia zhejiangensis
Caballeronia glebae
Trinickia clade (7)
Burkholderia s.s. clade (35)
Paraburkholderia oxyphila clade (22)
Paraburkholderia phosphatilytica
Paraburkholderia terrae clade (12)
Paraburkholderia megapolitana
Paraburkholderia sartisoli
Paraburkholderia phenazinium
Paraburkholderia susongensis
Paraburkholderia monticola
Paraburkholderia sprentiae
Paraburkholderia tuberum
Paraburkholderia atlantica
Paraburkholderia youngii
Ca. Paraburkholderia dryadicola Vdry
Ca. Paraburkholderia dryadicola Vmac
Paraburkholderia phytofirmans clade (21)
Paraburkholderia graminis
Ca. Paraburkholderia soutpansbergensis
Paraburkholderia phenoliruptrix
Paraburkholderia phenoliruptrix VmadMBG
Paraburkholderia phenoliruptrix VmadEBG
Paraburkholderia phenoliruptrix Vesc
Paraburkholderia phenoliruptrix Vran
Paraburkholderia phenoliruptrix VmadSA
Paraburkholderia phenoliruptrix Vinf
Paraburkholderia rhynchosiae
Paraburkholderia dilworthii
Paraburkholderia kirstenboschensis
Paraburkholderia caledonica
Paraburkholderia caledonica Vpyg08
Paraburkholderia caledonica Vpyg88
Paraburkholderia strydomiana
Paraburkholderia caledonica R-49542
Paraburkholderia caledonica R-82532
Tree scale: 0.1
B
Genome size (Mbp)
Tree scale: 0.1
Ca. Burkholderia crenata UZHbot9
Ca. Burkholderia crenata Avir
Ca. Burkholderia ardisicola Amam
Ca. Burkholderia ardisicola Acor
Ca. Burkholderia punctata
Ca. Burkholderia hochstetteri
Ca. Burkholderia schumanniana
Ca. Burkholderia kirkii
Ca. Burkholderia humilis
Ca. Burkholderia pumila
Ca. Burkholderia verschuerenii
Ca. Burkholderia umbellata
Ca. Burkholderia brachyanthoides
Ca. Paraburkholderia dryadicola Vmac
Ca. Paraburkholderia dryadicola Vdry
Paraburkholderia caledonica R-49542
Paraburkholderia caledonica R-82532
Paraburkholderia caledonica Vpyg08
Paraburkholderia caledonica Vpyg88
Ca. Paraburkholderia soutpansbergensis
Paraburkholderia phenoliruptrix VmadBGE
Paraburkholderia phenoliruptrix VmadMBG
Paraburkholderia phenoliruptrix VmadSA
Paraburkholderia phenoliruptrix Vinf
Paraburkholderia phenoliruptrix Vran
Paraburkholderia phenoliruptrix Vesc
2.65
2.58
4.38
3.95
3.91
3.5
3.62
4.01
5.32
3.7
6.15
4.22
3.75
4.31
4.29
8.92
8.71
7.45
7.44
5.18
4.76
4.77
5.03
5.01
4.98
4.99

Figure 1

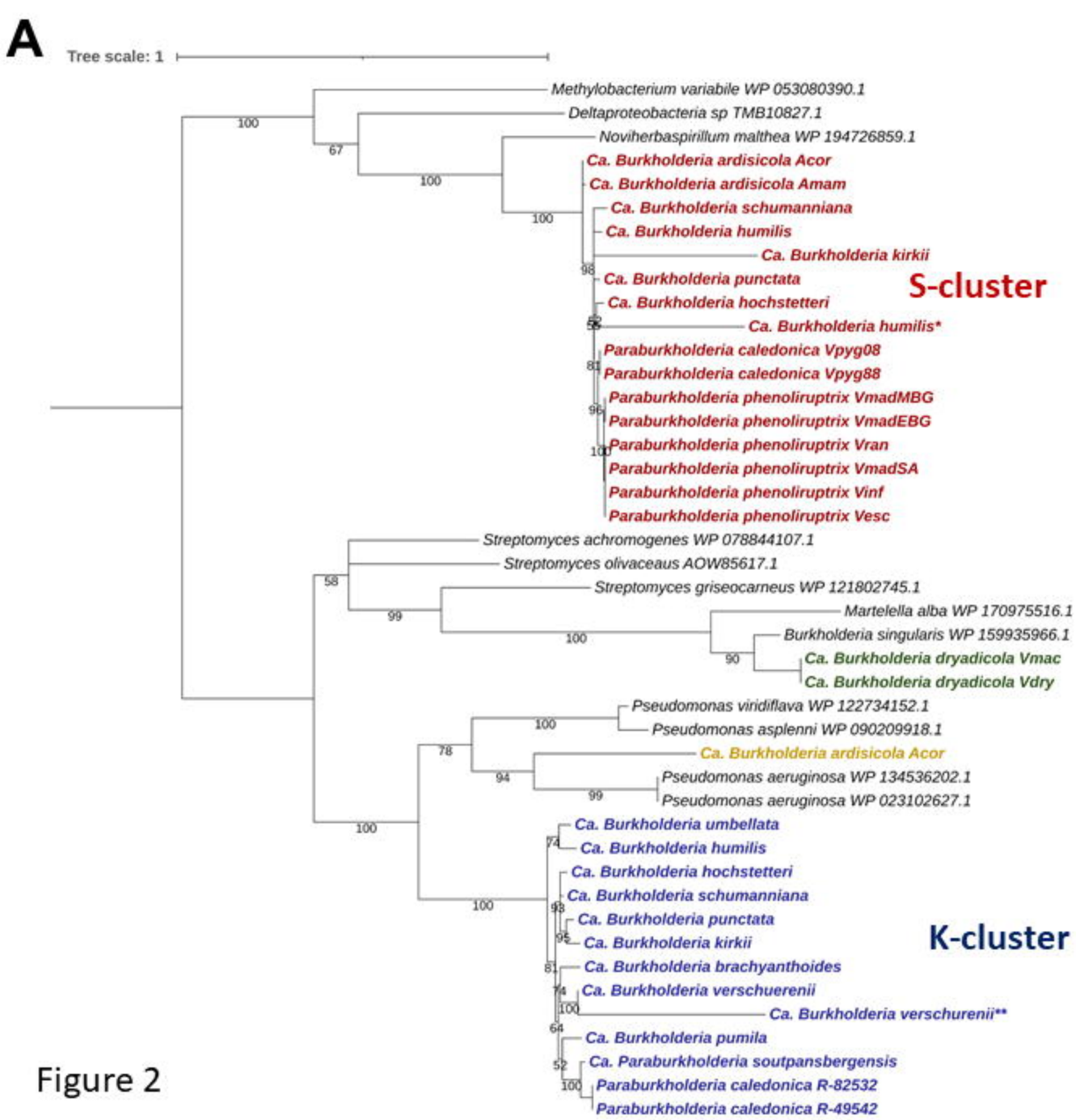
A
Tree scale: 1
Methylobacterium variabile WP 053080390.1
Deltaproteobacteria sp TMB10827.1
Noviherbaspirillum malthea WP 194726859.1
Ca. Burkholderia ardisicola Acor
Ca. Burkholderia ardisicola Amam
Ca. Burkholderia schumanniana
Ca. Burkholderia humilis
Ca. Burkholderia kirkii
Ca. Burkholderia punctata
Ca. Burkholderia hochstetteri
Ca. Burkholderia humilis*
Paraburkholderia caledonica Vpyg08
Paraburkholderia caledonica Vpyg88
Paraburkholderia phenoliruptrix VmadMBG
Paraburkholderia phenoliruptrix VmadEBG
Paraburkholderia phenoliruptrix Vran
Paraburkholderia phenoliruptrix VmadSA
Paraburkholderia phenoliruptrix Vinf
Paraburkholderia phenoliruptrix Vesc
S-cluster
Streptomyces achromogenes WP 078844107.1
Streptomyces olivaceaus AOW85617.1
Streptomyces griseocarneus WP 121802745.1
Martelella alba WP 170975516.1
Burkholderia singularis WP 159935966.1
Ca. Burkholderia dryadicola Vmac
Ca. Burkholderia dryadicola Vdry
Pseudomonas viridiflava WP 122734152.1
Pseudomonas asplenni WP 090209918.1
Ca. Burkholderia ardisicola Acor
Pseudomonas aeruginosa WP 134536202.1
Pseudomonas aeruginosa WP 023102627.1
Ca. Burkholderia umbellata
Ca. Burkholderia humilis
Ca. Burkholderia hochstetteri
Ca. Burkholderia schumanniana
Ca. Burkholderia punctata
Ca. Burkholderia kirkii
Ca. Burkholderia brachyanthoides
Ca. Burkholderia verschuerenii
Ca. Burkholderia verschurenii**
Ca. Burkholderia pumila
Ca. Paraburkholderia soutpansbergensis
Paraburkholderia caledonica R-82532
Paraburkholderia caledonica R-49542
K-cluster

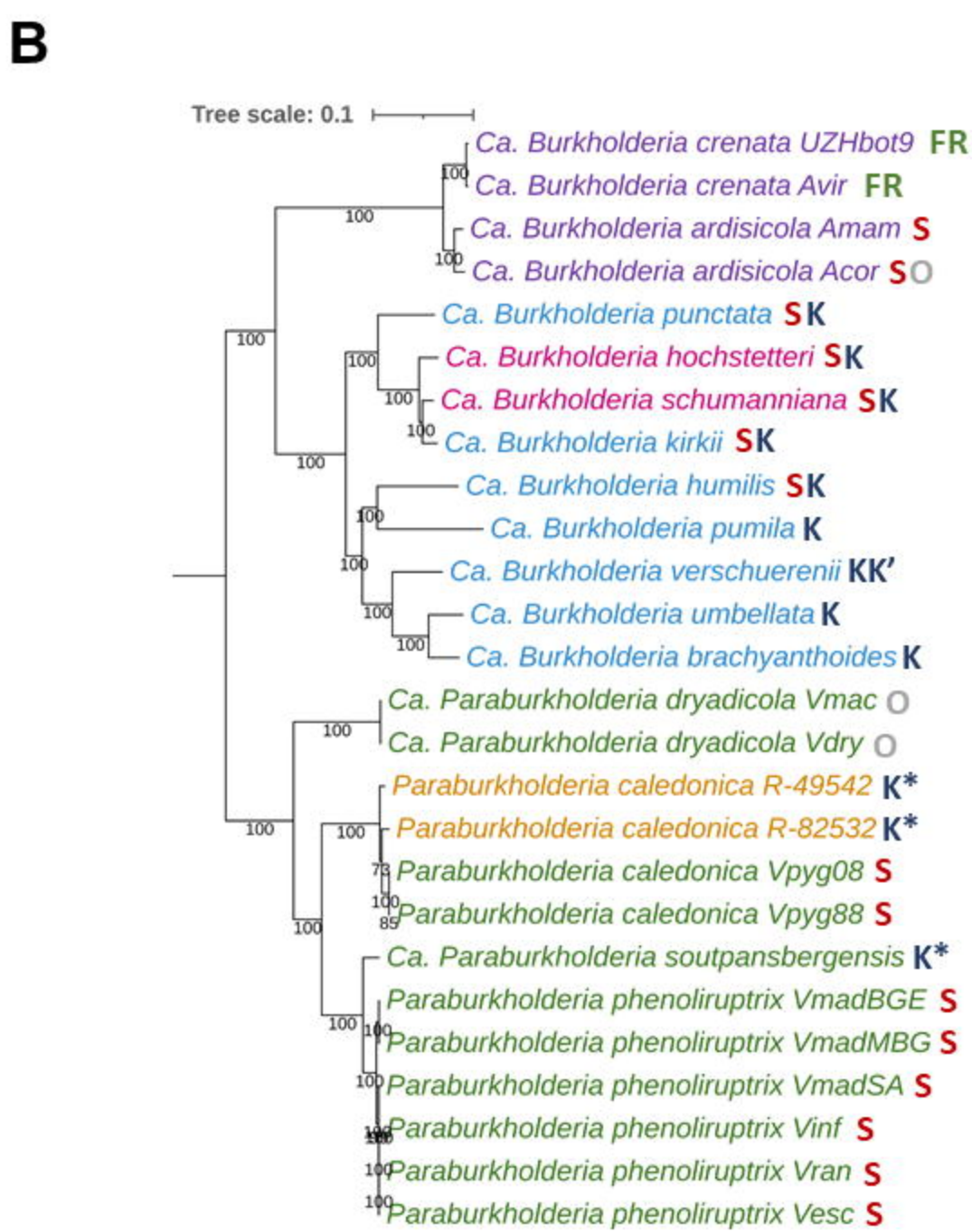
B
Tree scale: 0.1
Ca. Burkholderia crenata UZHbot9 FR
Ca. Burkholderia crenata Avir FR
Ca. Burkholderia ardisicola Amam S
Ca. Burkholderia ardisicola Acor SO
Ca. Burkholderia punctata SK
Ca. Burkholderia hochstetteri SK
Ca. Burkholderia schumanniana SK
Ca. Burkholderia kirkii SK
Ca. Burkholderia humilis SK
Ca. Burkholderia pumila K
Ca. Burkholderia verschuerenii KK'
Ca. Burkholderia umbellata K
Ca. Burkholderia brachyanthoides K
Ca. Paraburkholderia dryadicola Vmac O
Ca. Paraburkholderia dryadicola Vdry O
Paraburkholderia caledonica R-49542 K*
Paraburkholderia caledonica R-82532 K*
Paraburkholderia caledonica Vpyg08 S
Paraburkholderia caledonica Vpyg88 S
Ca. Paraburkholderia soutpansbergensis K*
Paraburkholderia phenoliruptrix VmadBGE S
Paraburkholderia phenoliruptrix VmadMBG S
Paraburkholderia phenoliruptrix VmadSA S
Paraburkholderia phenoliruptrix Vinf S
Paraburkholderia phenoliruptrix Vran S
Paraburkholderia phenoliruptrix Vesc S

Figure 2